# Effect of Spacer Length between Consecutive Bends on Friction Factors of U-Type Wavy Tubes

A Thesis Submitted

by

MD. SULTAN SALAUDDIN

Student No.0409102082

**Department Of Mechanical Engineering**
Bangladesh University of Engineering & Technology
Dhaka, Bangladesh

**March 2013**

# Effect of Spacer Length between Consecutive Bends on Friction Factors of U-Type Wavy Tubes

A thesis

Submitted to

Department of Mechanical Engineering

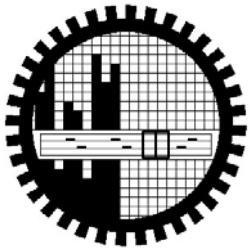

Bangladesh University of Engineering and Technology.

by

MD. SULTAN SALAUDDIN

Student No: 0409102082

Under the supervision of

Dr. M. Mahbubur Razzaque
Professor, Department of Mechanical Engineering
Bangladesh University of Engineering and Technology Dhaka, Bangladesh.

In partial fulfillment of the requirement for the degree of Master of Science in Mechanical Engineering.

March 2013

# RECOMMENDATION OF THE BOARD OF EXAMINERS

The board of examiners, hereby, recommends to the Department of Mechanical Engineering, BUET, Dhaka, the acceptance of this thesis titled **"Effect of Spacer Length between Consecutive Bends on Friction Factors of U-Type Wavy Tubes,"** submitted by Md. Sultan Salauddin, student no: 0409102082, in partial fulfillment of the requirements for the degree of Master of Science in Mechanical Engineering.

Chairman (Supervisor) : _____

Dr. M. Mahbubur Razzaque
Professor
Department of Mechanical Engineering
BUET, Dhaka, Bangladesh.

Member (Ex-officio) : _____

Dr. Md. Ehsan
Professor & Head
Department of Mechanical Engineering
BUET, Dhaka, Bangladesh.

Member : _____

Dr. Mohammad Ali
Professor
Department of Mechanical Engineering
BUET, Dhaka, Bangladesh.

Member : _____

Dr. S. Reaz Ahmed
Professor
Department of Mechanical Engineering
BUET, Dhaka, Bangladesh.

Member (External) : _____

Dr. A. K. M. Sadrul Islam
Professor
Department of MCE, IUT, Dhaka.

# ACKNOWLEDGEMENT

The author would like to express his appreciation and gratitude to Professor Dr. M. Mahbubur Razzaque, Department of Mechanical Engineering, Bangladesh University of Engineering and Technology, for providing the opportunity to work with him as well as for his care during this thesis endeavor. As a supervisor, he has constantly guided the author to remain focused on achieving the goal. His observations and comments tremendously helped in establishing the overall direction of the thesis and to move forward with investigation in depth.

The author gratefully acknowledges the support of the technicians of the fluid mechanics laboratory of Mechanical Engineering Department for providing required experimental facilities. The author is also thankful to the instructors, the operators and the technicians of different laboratories and workshops for their help during the development and fabrication of the experimental setup.

The author also would like to thank all coworkers for their encouragement and help during the course of this work.

# TABLE OF CONTENTS


**Page number**

Recommendation of the Board of Examiners ii

Acknowledgement iii

List of tables vi

List of figures vii

Abstract x

Nomenclature xi

## CHAPTER 1: INTRODUCTION

1.1 Application of U-type Wavy Tubes 1

1.2 Flow through U-type Wavy Tubes 3

1.3 Background and Literature Survey 4

1.3.1 Flow through bent pipes and curved tubes 4

1.3.2 Flow through return bends or U-bends 5

1.3.3 Flow through wavy and corrugated tubes 6

1.3.4 Flow through U-type wavy tubes 6

1.4 Objectives of the present thesis 9

## CHAPTER 2: EXPERIMENTAL STUDY

2.1 Introduction 10

2.2 Experimental Setup 10

2.2.1 Test Section 11

2.2.2 Centrifugal pump 13

2.2.3 Gate Valves 14

2.2.4 Water Tank 15

2.2.5 Measuring Flask 15

**Page number**


2.2.6 Wooden Frame 15
2.2.7 U-tube mercury manometer 16
2.2.8 Socket Reducer 17
2.2.9 T-joint 17
2.2.10 Flow control valve 18
2.3 Experimental Procedure 19
2.4 Test Condition 20
2.5 Uncertainty analysis 21

**CHAPTER 3: RESULTS AND DISCUSSION**

3.1 Introduction 22
3.2 Parameters considered 22
3.3 Data collection and calculation procedure 22
3.4 Verification of Experimental Data 27
3.5.1 Effects of Spacer Length 28
3.5.2 Dimensionless Critical Spacer Length Ratio, $L_{cr}$ 32
3.5.3 Effects of Number of Bends 36
3.5.4 Effects of number of bends on bend friction factor and critical spacer length ratio 39

**CHAPTER 4: CONCLUSION**

4.1 Major Outcomes 45
4.2 Scope for Future Work 46

REFERENCE 47
APPENDIX-A 51
APPENDIX-B 62

# LIST OF TABLES


| | | Page no. |
|---|---|---|
| **Table 2.1** | Pump specification | 13 |
| **Table 2.2** | Uncertainty in measured values at $Re > 20000$ | 21 |
| **Table 3.1** | Experimental data and results | 26 |
| **Table 3.2** | Bend friction factors for different $L/d$ ratio and Reynolds number ($n = 9$) | 33 |
| **Table 3.3** | Bend friction factors for different $L/d$ ratio and Reynolds number ($n = 15$) | 40 |
| **Table A.1** | Experimental data for Spacer Length = 2R, Curvature Radius = 25.4mm, Number of bend = 15 | 51 |
| **Table A.2** | Experimental data for Spacer Length = 3R, Curvature Radius = 25.4mm, Number of bend = 15 | 52 |
| **Table A.3** | Experimental data for Spacer Length = 4R, Curvature Radius = 25.4mm, Number of bend = 15 | 53 |
| **Table A.4** | Experimental data for Spacer Length = 4R, Curvature Radius = 25.4mm, Number of bend = 13 | 54 |
| **Table A.5** | Experimental data for Spacer Length = 4R, Curvature Radius = 25.4mm, Number of bend = 11 | 55 |
| **Table A.6** | Experimental data for Spacer Length = 4R, Curvature Radius = 25.4mm, Number of bend = 9 | 56 |
| **Table A.7** | Experimental data for Spacer Length = 3R, Curvature Radius = 25.4mm, Number of bend = 9 | 57 |
| **Table A.8** | Experimental data for Spacer Length = 2R, Curvature Radius = 25.4mm, Number of bend = 9 | 58 |
| **Table A.9** | Experimental data for Spacer Length = R, Curvature Radius = 25.4mm, Number of bend = 9 | 59 |

# LIST OF FIGURES


| | | Page no. |
|---|---|---|
| Figure 1.1 | U-type wavy tube with fins on its surface (left) and condenser coils (right). | 1 |
| Figure 1.2 | Various types of heat exchangers using U-type wavy tubes | 2 |
| Figure 1.3 | U-type wavy tubes: without spacer (left) and with spacer (right) | 2 |
| Figure 2.1 | Complete view of the experimental setup | 11 |
| Figure 2.2 | Schematic diagram of the experimental setup | 12 |
| Figure 2.3 | The centrifugal pump used for circulating water through the test section | 13 |
| Figure 2.4 | Gate valve V-1 for flow rate control | 14 |
| Figure 2.5 | Water tank connected to the pump for supplying water to the test section | 14 |
| Figure 2.6 | The wooden frame to form U-type wavy configuration of the flexible tube | 15 |
| Figure 2.7 | U-Tube Mercury manometer | 16 |
| Figure 2.8 | Valves and joints at the top of the manometer | 16 |
| Figure 2.9 | Socket Reducer. | 17 |
| Figure 2.10 | T- joint | 17 |
| Figure 2.11 | Flow control valve | 18 |

| | | |
|---|---|---|
| Figure 2.12 | Connection of different fittings and valves with the flexible tube | 18 |
| Figure 2.13 | Measurement of volume flow rate | 20 |
| Figure 3.1 | Schematic diagram of the experimental setup showing the pressure taping points | 23 |
| Figure 3.2 | Bend friction factor, $f_B$ and straight friction factor $fs$ vs. Reynolds number,$Re$. Experimental data and predictions by Blasius Equation | 27 |
| Figure 3.3 | Bend friction factor, $f_B$ vs Reynolds number, $Re$ for number of bend, $n$=9 and spacer length, $L = R$ | 28 |
| Figure 3.4 | Bend friction factor, $f_B$ vs Reynolds number, $Re$ for number of bend, $n$=9 and spacer length, $L = 2R$ | 29 |
| Figure 3.5 | Bend friction factor, $f_B$ $vs$ Reynolds number, $Re$ for number of bend, $n$ = 9 and spacer length, $L = 3R$. | 29 |
| Figure 3.6 | Bend friction factor, $f_B$ vs Reynolds number, $Re$ for number of bend, $n$ = 9 and spacer length, $L = 4R$ | 30 |
| Figure 3.7 | Bend friction factor, $f_B$ vs Reynolds number, $Re$ for different spacer lengths, $L$ | 31 |
| Figure 3.8 | Bend friction factor, $f_B$ vs Dean Number, $D_n$ for different spacer lengths | 31 |
| Figure 3.9 | Bend friction factor, $f_B$ vs Reynolds Number, for various spacer length ratio ($L/d$). | 32 |
| Figure 3.10 | Bend friction factor, $f_B$ vs dimensionless spacer length ($L/d$) for number of bend ($n$ = 9) and Reynolds number ($Re$ = 3702) | 34 |
| Figure 3.11 | Bend friction factor, $f_B$ vs dimensionless spacer length ($L/d$) for number of bend ($n$ = 9) and Reynolds number ($Re$ = 8000) | 34 |
| Figure 3.12 | Bend friction factor, $f_B$ vs dimensionless spacer length ($L/d$) for number of bend ($n$ = 9) and Reynolds number ($Re$ = 11695) | 35 |
| Figure 3.13 | Bend friction factor, $f_B$ vs dimensionless spacer length ($L/d$) for number of bend ($n$ = 9) and Reynolds number ($Re$ = 18088) | 35 |
| Figure 3.14 | Bend friction factor, $f_B$ vs dimensionless spacer length | 36 |
| Figure 3.15 | Bend friction factor, $f_B$ vs Reynolds number, $Re$ for number of bend, n = 9 and spacer length , $L = 4R$ | 37 |

| | | |
|---|---|---|
| Figure 3.16 | Bend friction factor, $f_B$ vs Reynolds number, *Re* for number of bend $n$ = 11 and spacer length, $L = 4R$ | 37 |
| Figure 3.17 | Bend friction factor, $f_B$ vs Reynolds number, *Re* for number of bend, $n$ = 13 and spacer length, $L = 4R$ | 38 |
| Figure 3.18 | Bend friction factor, $f_B$ vs Reynolds number, Re for number of bend, $n$ = 15 and spacer length, $L = 4R$ | 38 |
| Figure 3.19 | Effects of number of bends on the bend friction factor in the U-type wavy tube | 39 |
| Figure 3.20 | Bend friction factor, $f_B$ vs Reynolds Number (*Re*) for various spacer lengths | 40 |
| Figure 3.21 | Bend friction factor, $f_B$ vs dimensionless spacer length (*L/d*) for number of bend (n = 15) and Reynolds number (*Re* = 3780). | 41 |
| Figure 3.22 | Bend friction factor, $f_B$ vs dimensionless spacer length (*L/d*) for number of bend ($n$ = 15) and Reynolds number (*Re* = 10953). | 41 |
| Figure 3.23 | Bend friction factor, $f_B$ vs dimensionless spacer length (*L/d*) for number of bend ($n$ = 15) and Reynolds number (*Re* = 12763). | 42 |
| Figure 3.24 | Bend friction factor, $f_B$ vs dimensionless spacer length (*L/d*) for number of bend ($n$ = 15) and Reynolds number (*Re* = 15631) | 42 |
| Figure 3.25 | Bend friction factor, $f_B$ vs dimensionless spacer length (*L/d*) for $n$ = 15 | 43 |
| Figure 3.26 | Nusselt number, $Nu_d$ vs spacer length ratio, *x/d* for different values Reynolds number, *Re*. | 44 |

# ABSTRACT

U-type wavy tubes are used in a great number of heat transfer equipment and flow transmitting devices. It provides a long flow path in a relatively small space and thereby allows the fluid flowing through the tube to have sufficient time for heat and mass transfer. Besides, vigorous mixing of fluid provided by the alternating bends enhances the heat and mass transfer processes. During fluid flow in U-type wavy tubes through consecutive bends, the flow phenomenon becomes more complex and the head loss increases.

The present thesis work is undertaken to experimentally measure the head loss and the friction factor in U-type wavy tubes. A test rig has been designed and fabricated to determine the friction factor for small diameter flexible tubes of U-type wavy configuration using water as the working fluid. Experiments are done by varying the number of bends and the spacer length to study their effects on the bend friction factor. The range of the Reynolds number is 1000 to 23,500 and that of Dean number is 500 to 7000.

It has been found that the bend friction factor decreases with the increase of Reynolds Numbers. At large values of Reynolds number, the differences in bend friction factors due to variations in spacer lengths or number of bends diminishes. The bend friction factor increases with the increase of the spacer length up to a certain value of the spacer length ratio. Beyond this value of the spacer length ratio, the bend friction factor stops changing. This spacer length ratio is termed as the critical spacer length ratio. In these experiments, the dimensionless critical spacer length ratio is found to be 15.2. This value of critical spacer length ratio is not affected by the number of bends

The outcome of this study will be useful in designing fluid flow through U- type wavy tubes in various kinds of heat transfer equipment.

# NOMENCLATURE

| | |
|---|---|
| $D_n$ | Dean number |
| $d$ | Diameter of flexible tube |
| $f_B$ | Bend friction factor |
| $f_S$ | Straight friction factor |
| $H$ | Manometer reading |
| $L$ | Spacer Length |
| $L_c$ | Curved Length of a U bend |
| $L_{cr}$ | Critical spacer length ratio |
| $L_{st}$ | Straight Length |
| $N$ | Number of bends |
| $\Delta P_T$ | Total pressure drop |
| $Q$ | Volume flow rate |
| $R$ | Radius of curvature of the bends |
| $Re$ | Reynolds number |
| $S_g$ | Specific gravity of mercury |
| $S_w$ | Specific gravity of water |
| $V$ | Volume |
| $\mu$ | Absolute or dynamic viscosity |
| $v$ | Velocity of water |
| $\rho$ | Density of water |

# CHAPTER 1

# INTRODUCTION

In various types of heat and mass transfer equipment, the process is sometimes enhanced by increasing the heat or mass transfer area, sometimes by increasing the residence or contact time and sometimes by increasing both. There are various ways to implement these principles. Using fins, coils and U-type wavy tubes, as shown in Fig.1.1, are some popular techniques for implementing these principles. This thesis is concerned with U-type wavy tubes.

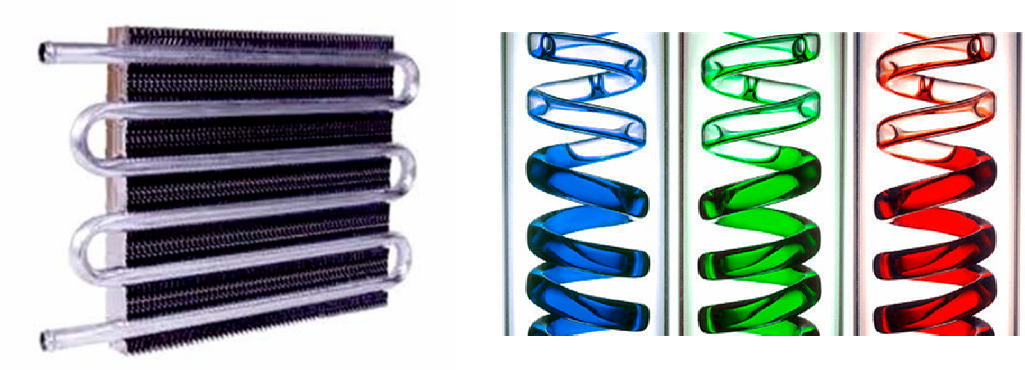

Figure 1.1: U-type wavy tube with fins on its surface (left) and condenser coils (right).

## 1.1: Application of U-type wavy tubes

U-type wavy tubes are used in a great number of heat transfer equipment and flow transmitting devices. It provides a long flow path in a relatively small space and thereby allows the fluid flowing through the tube to have sufficient time for heat and mass transfer. Besides, vigorous mixing of fluid provided by the alternating bends enhances the heat and mass transfer processes. The wavy tubes are used in shell and tube heat exchanger for domestic and industrial water heating systems and in plate solar collectors. Other

applications include condensers, evaporators, super-heaters, chemical and nuclear reactors, etc. Figure 1.2 shows various types of heat exchangers utilizing U-type wavy tubes.

Figure 1.2: Various types of heat exchangers using U-type wavy tubes.

The use of small diameter tubes in the application of the HVAC-R (Heating, Ventilation, Air conditioning and Refrigeration) is very popular because of less refrigerant storage, better air-side heat transfer and smaller air side drag. The U-type wavy tubes in an air cooled heat exchanger sometimes have a spacer section between two consecutive 180° return bends while sometimes the tube is made simply undulated without any spacer between consecutive bends. Because of their wide application in heat exchangers, it is necessary to understand the behavior of flow through U-type wavy tubes.

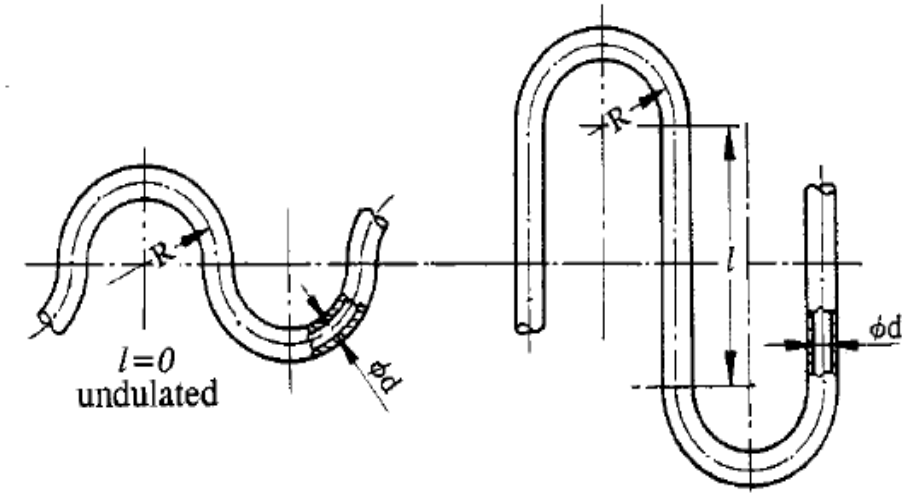


Figure 1.3: U-type wavy tubes: without spacer (left) and with spacer (right).

### 1.2: Flow though U-type wavy tubes

When a fluid flows through a stationary curved pipe, a pressure gradient across the pipe is required to balance the centrifugal force arising from the curvature. If the pipe is lying on a horizontal plane, the fluid velocity near the top and the bottom of the pipe is slower than the fluid velocity along the center line of the pipe. It requires a small pressure gradient to balance the centrifugal force. In consequence, a flow is set up in which the fluid near the top and the bottom moves inwards and the fluid in the middle moves outwards. This flow is known as the secondary flow. The secondary flow is superposed on the main stream, so that the resultant flow is helical at the top and bottom halves of the pipe. As a result of the secondary flow, the region of maximum velocity in the main stream is shifted towards the outer part of the wall, the total frictional loss of energy near the wall of the pipe increases, and the flow experiences more resistance in passing through the pipe. This increase in resistance is small when the curvature of the pipe is small. If the curvature is significant the axial velocity distribution is entirely altered by the secondary flow and a considerable resistance is observed. The first theoretical study of the subject was made by Dean [Shames, 1992, Ward-Smith, 1980], who pointed out that the dynamic similarity of the flow depends on a non-dimensional parameter,

$$D_n = \frac{\rho V d}{\mu}\sqrt{\frac{d}{2R}} = \mathrm{Re}\sqrt{\frac{d}{2R}} \qquad 1.1$$

Where $D_n$ is called the "Dean Number", $Re$ is the Reynolds number, $V$ is the mean velocity along the pipe, $\mu$ is the coefficient of dynamic viscosity and $d$ is the diameter of the pipe which is bent into a circle of radius $R$. The increase of friction factor due to bending depends only on the Dean number, $D_n$, as long as the motion is laminar. But that is no longer the case when turbulence sets in. At higher Dean Number a centrifugal instability near the concave outer wall of the pipe gives the origin of a developing additional pair of vortices called "Dean Vortices". Flow in a wavy pipe approaching a consecutive bend is much more complex. Pressure losses of the flow are a result of the very complex velocity gradient distribution and friction at the pipe wall and of the dissipation of energy of the vortex pairs produced by each consecutive bend.

## 1.3: Background and Literature Survey

### 1.3.1: Flow through bent pipes and curved tubes

Apart from the pioneer work of Dean in 1927, many researchers paid attention to understand the frictional performances of bends. Among others, Ito's [1960] work on the pressure loss in smooth pipe bends is one of the old works in this area. He conducted experimental studies to determine the pressure losses for turbulent flow in smooth pipe bends of circular cross section. Manlapaz and Churchill [1980] worked on fully developed laminar flow in a helical coiled tube of finite pitch. Ward-Smith [1980] studied the dynamics of internal fluid flow in pipes and ducts. Shimizu *et al.* [1982] performed a study on hydraulic loss and flow pattern in bent pipes and compared their results in wavy pipes and quasi-coiled tubes. Von and Wilson [1989] proposed a universal resistance correlation for friction factor, Reynolds number and roughness height for the entire range of turbulent flow in pipes covering all regimes. Reno *et al.* [1983] measured the relative roughness for mineral porous media. A method for the experimental determination of the internal diameter and the equivalent roughness was proposed for different commercial membranes used in ultra filtration and microfiltration processes. The main results were the estimation of the hydraulic diameter of tubular membranes in order to predict friction factors and the equivalent roughness.

The flow through a curved tube whose radius of curvature varies with time was studied by Aland *et al.* [1998] in order to better understand the flow patterns in coronary arteries. A computational flow model was constructed using commercially available software. The artery model assumed a uniform circular cross section, and the curvature was considered to be constant along the tube. Lynch *et al.* [1996] studied the flow in a tube with non-uniform, time-dependent curvature in connection with the analysis of blood flow in the major coronary arteries, which are situated on the outer surface of the pumping heart. Heat transfer and pressure loss in helically coiled tubes with turbulent flow were studied by Rogers and Mayhew [1964] whereas, heat transfer and friction factor characteristics of laminar flow through a circular tube fitted with helical screw-tape inserts were experimentally investigated by Sivashanmugam and Suresh [2006].

### 1.3.2 Flow through return bends or U-bends

Chen and his coworkers performed a series of studies on the frictional performance of two phase flows through return bends. In 2001, Chen *et al.* [2001] investigated two-phase frictional pressure drop of air-water in small horizontal tubes. Following that, they [Chen *et al.*, 2002] studied the influence of horizontal return bends on the two-phase flow pattern in a 6.9 mm diameter tube and developed an empirical correlation. Yutasak and Somchai [2005] investigated the effect of fin pattern on the air-side performance of herringbone wavy fin-and-tube heat exchangers. The experiments have been performed to determine the effects of fin patterns and edge corrugations on the air-side performance of the heat exchangers. Domanski and Hermes [2006] proposed a new correlation for two-phase flow pressure drop in 180° return bends based on experimental data for R-22 and R-410a from two independent studies. They experimented with smooth tubes of inner diameters from 3.3 mm to 11.6 mm, bend radii from 6.4 mm to 37.3 mm and curvature ratios from 2.3 to 8.2. The correlation incorporates a two-phase pressure drop for straight tubes and a multiplier that accounts for the bend curvature.

Cho and Tae [2001] investigated about the condensation and evaporation heat transfer coefficient of R-22 and R-407C inside a micro fin tube with a U-bend. Their result showed that the condensation and evaporation heat transfer of a straight section downstream the U-bend is 33% higher than that of a straight section upstream the U-bend. Chen *et al.* [2004] presented single-phase and two-phase friction factor data for R-410a in four U-type return bends with tube diameters 3.3 and 5.07 mm and curvature ratio ranged from 3.91 to 8.15. The friction factor and the two-phase pressure gradient in the return bend considerably increase with the decrease of curvature ratio. For the single-phase results, existing correlations gave fair agreements with the presented data. For two-phase results, the Geary correlation showed a better agreement with the data. A modified two-phase friction factor based on the Geary correlation was then proposed. The proposed correlation gave a good agreement to the experimental data with a mean deviation of 19.1%.

### 1.3.3 Flow through wavy and corrugated tubes

Heat transfer and flow through wavy and corrugated tubes of different arrangement were also studied in connection to the studies of heat exchangers. Ciofalo and Piazza [2000] investigated the flow and heat transfer in corrugated-undulated plate heat exchangers. James *et al.* [1990] performed experiments with flow of a test fluid in corrugated tubes. Measurements of flow resistance in several corrugated tubes were made with the test fluid at Reynolds numbers less than unity. Wang *et al.* [2003] examined the influence of return bend on the frictional performance of R-410a and R-22 in a 5-mm diameter tube of a curvature ratio of 6.63. Huzarewicz and Gupta [1991] investigated experimentally the effects in flow of fluids through sinusoidal wavy tubes. Popiel and Merwe [1996] measured pressure loss in a sine-waved hydraulically smooth pipe. The effect of the dimensionless wave-length and amplitude on the Darcy friction factor was investigated in the range of the Reynolds number from about 100 to 10 000 for various values of wavelength and amplitude.

### 1.3.4 Flow through U-type wavy tubes

During fluid flow in U-type wavy tubes through consecutive bends, the flow phenomenon becomes more complex and the head loss increases. Chen *et al.* [2008] performed experiments with U-type wavy tubes in horizontal and vertical arrangements and measured two-phase frictional pressure drop. Popiel and Wojtkowiak [2000] conducted an experimental study with U-type undulated pipe flow of fluids such as air and water. They gave empirical correlation for estimating friction factor, i.e. head loss in U-type wavy tubes based on measurements of pressure losses in a hydraulically smooth U-type or undulated tube. The effect of the dimensionless curvature radius $2R/d$ on the Darcy friction factor was investigated in the range of the Reynolds number from about 50 to 10,000 and for the dimensionless pipe curvature radii $2R/d$ = 5.62, 7.95, 11.13, 16.03, 22.58, and 27.85. A smooth transition from laminar to turbulent regime in the friction factor versus Reynolds number plot, typical for a curved pipe flow, was observed. The experimental data were correlated with the relatively simple equation using New Dean Number: $D_n' = Re^*(d/2R)$, as

$$ln\left(f_w \frac{Re}{64}\right) = a + b\left(ln\, D'_n\right)^2 \;; \quad \text{a = 0.021796; b = 0.0413356} \qquad 1.2$$

However, this is not valid for larger values of $D'_n$ and *2R/d*, e.g., for $D'_n > 200$ at *2R/d* = 22.58, and for $D'_n > 70$ at *2R/d* = 27.85. They also noticed that the influence of the pipe curvature was insignificantly small for values of the New Dean number smaller than 3. This correlation has limitations and is applicable only within the range of their data and fail to predict pressure drop at large Reynolds numbers. Wojtkowiak and Popiel [2000] also investigated the effect of cooling on pressure losses in U-type wavy pipe flow.

Chen *et al.* [2003] measured the pressure drop and investigated the frictional performance of water flowing through small diameter tubes having U-type wavy configuration. They also gave empirical correlation for estimating friction factor, i.e. head loss in U-type wavy tubes based on measurements. The inner diameters of the test copper tubes were 3.43, 5.07, and 8.29 mm, whereas the curvature radii (*2R/d*) and spacer length (*L/d*) spanned from 3.75 to 7.87 and 1.93 to 7.0, respectively. The tests were carried out with water in the range, $200 < Re < 18000$. The measured pressure loss in U-type wavy tube include the loss in U-bends and the loss caused by the distorted flow in the downstream straight tube. Thus, an equivalent friction factor termed as bend friction factor, $f_B$ is defined. For both laminar and turbulent flow, the bend friction factor depends on the dimensionless curvature ratio and dimensionless spacer length. The test results indicated that the correlations proposed by Popiel and Wojkowiak [2000] cannot predict their data. They proposed a new correlation for predicting friction factor based on the experimental data of characteristic parameters like curvature ratio, spacer length, New Dean Number and Reynolds number. A good agreement with a mean standard deviation of 5.6% was claimed between the proposed correlation and the existing data, which included their own data and the data from Popiel and Wojtkowiak (2000). These correlations also have limitations and are applicable only within the range of their data and fail to predict at large Reynolds numbers. Later, influence of the presence of oil on R-410a two-phase frictional pressure drop in a small U-type wavy tube was studied by Chen *et al.* [2005].

Das *et al.* [2007] measured pressure drop in both straight section and bend section for water flowing in small diameter tubes having U-type wavy configuration and proposed a correlation which is dependent on spacer length, number of bends, curvature ratio. The test was done in the turbulent regime. The curvature ratio (*2R/d*) spanned from 6.43 to 13.03 and the dimensionless spacer length (*L/d*) spanned from 3.16 to 6.41. The bend friction factor is found to decrease with increase in curvature ratio (*2R/d*) and dimensionless spacer length (*L/d*). The experimentally determined Fanning friction factor in the straight section was found to match closely with the well-known Blasius equation for the turbulent regime. Predicted friction factors were in good agreement with the experimental data with a mean standard deviation of only 4%.

Hamim *et al.* [2008] did experiments with water to determine friction factors for small diameter copper tubes of U-type wavy configuration. In one set of tests, the number of bends was varied (9, 11, 13 and 15) and in the other set, the inner diameter was varied (3.9, 4.85 and 7.9 mm). In these tests, the range of Reynolds number was 4000 to 30,000. The range of the dimensionless curvature ratio (*2R/d*) was 6.43 - 13.03 and of the dimensionless spacer length (*L/d*) was 3.16 - 6.41. An equivalent bend friction factor was defined considering only the pressure drop due to a bend. A generalized correlation considering the effects of dimensionless curvature ratio, dimensionless spacer length and number of bends was developed, which, in the limiting condition, reduces to Blasius equation for straight smooth tubes. Predicted friction factors were in good agreement with the experimental data. However their experimental data indicated that with the increment of spacer length the effect of number of bends diminishes.

Razzaque *et al.* [2010] and Hanif *et al.* [2011] used CFD technique for determination of friction factor for small diameter copper tubes of U-type wavy configuration. Simulations were done by varying number of bends, n (9-55), inner diameters, *d* (3.5-10 mm) & spacer length, *L* (0-50 mm). The curvature ratios (*2R/d*) and spacer length (*L/d*) spanned from 5.08 to 14.51 and 0 to 12.82, respectively. The test range of the Reynolds number for water was $200 < Re < 32{,}000$. The predicted pressure loss in U-type wavy tube includes the loss in U-

bends and the loss caused by the distorted flow in the downstream straight tube. Thus, an equivalent friction factor, $f_B$ was defined. After a certain spacer length, change of bend friction factor becomes independent of the number of bends and spacer length, which defines the critical spacer length. A simple correlation for both laminar and turbulent regime friction factors for U-type wavy tubes was developed based on the simulation results considering the effect of Dean number ($D_n$) and dimensionless spacer length ($L/d$) which, was in good agreement with both simulation and experimental data. They predicted that with increase of dimensionless spacer length ratio up to a certain limit, normally 10-11, friction factor increases. Increasing spacer length ratio beyond this value does not influence the friction factor much. However, their work was based on a two dimensional CFD simulation, whereas the real problem is a 3D one. Therefore, to validate the findings, it is essential to compare the simulation results with experimental data.

### 1.4 Objective of the present thesis

It has been reported in literature that friction factor due to consecutive U-bends keeps on increasing as the spacer length increases. However, this trend ceases after a certain spacer length and the friction factor becomes practically constant. This spacer length is termed as critical spacer length. The present thesis work is undertaken to fulfill the need of experimentally confirming the existence of the so-called critical spacer length. Specific objectives of this work are as follows:

i. To design and fabricate an experimental set-up for measuring pressure drop and friction factor in U- type wavy tubes.
ii. To measure pressure drop and calculate bend friction factors.
iii. To study the effect of spacer length and number of bends on bend friction factor and to experimentally determine the critical value of the dimensionless spacer length.

The outcome of this study will be useful in designing fluid flow through U- type wavy tubes in various kinds of heat transfer equipment.

# Chapter-2

# EXPERIMENTAL STUDY

## 2.1: Introduction

As mentioned in the previous chapter, the main objective of this work is to carry out an experimental study on the effect of spacer length and number of bends on bend friction factor and to determine the critical value of the dimensionless spacer length. So, an experimental setup is designed and fabricated for experiments of flow through U-type wavy tubes with the variation of flow rate, spacer length, number of bend and tube diameter. Water is used as the working fluid.

Several sets of test sections were prepared with variations of spacer length and number of bends. While testing the effect of spacer length and spacer length to diameter ratio, the spacer length ($L$) was varied but the diameter ($d$) and the radius of curvature ($R$) of the set of test sections were fixed. In case of testing the effect of number of bends only the number of bends is changed and others parameters were fixed.

## 2.2: Experimental Setup

A photograph of the experimental arrangement and the schematic diagram of the experimental setup are shown in Figures 2.1 and 2.2, respectively. The experimental setup consists of a water tank, a centrifugal pump, a gate-valve (V-1) for controlling the flow rate, valves for changing the flow direction, test section, pressure tappings, a U-tube mercury manometer for measuring the pressure drop and a volumetric flask for measuring

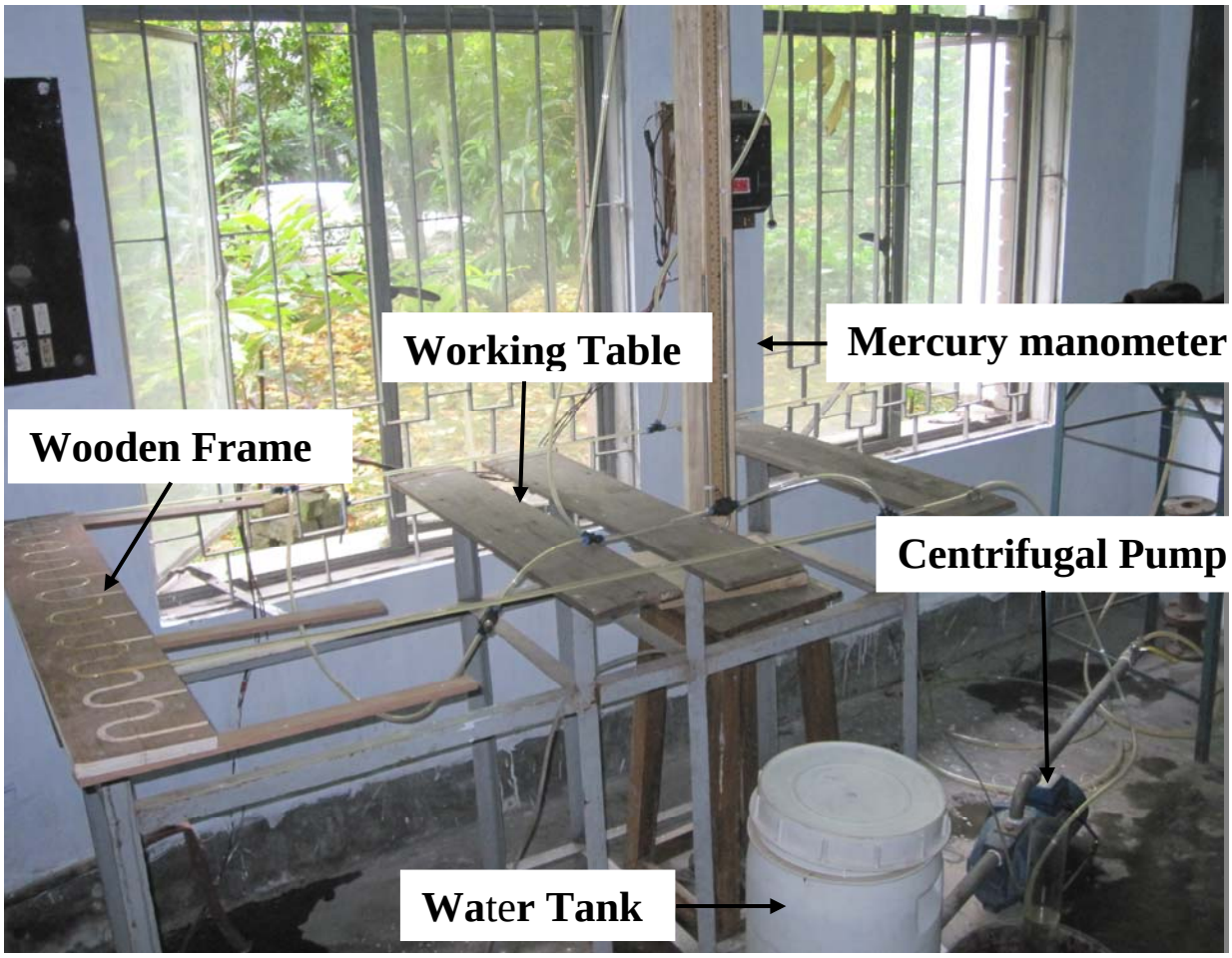


Figure 2.1: Complete view of the experimental setup.

the water flow rate. The detail description of the setup is provided in the following sections.

### 2.2.1 Test Section

The test sections were made of flexible tubes made of clear polyurethane. The U-type wavy patterns were formed by using a template made of wood. The templates were arranged in such a way that the spacer length could be adjusted while the radius of curvature was fixed.

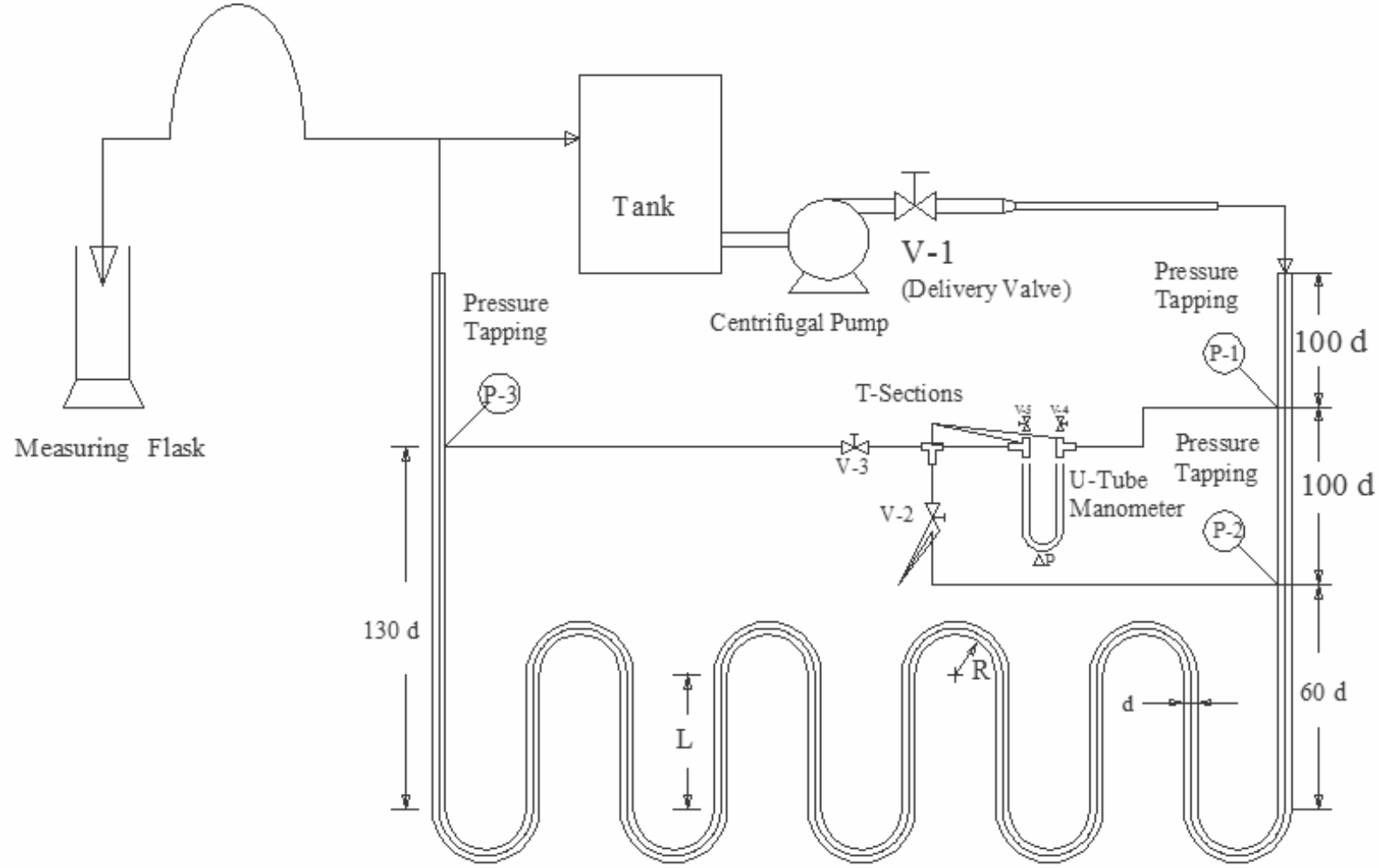


Figure-2.2: Schematic diagram of the experimental setup

### 2.2.2 Centrifugal pump

A centrifugal pump, shown in Fig. 2.3, was used to circulate water through the test section as well as the circuit. The flow rate was controlled by a gate valve (V- 1) attached to its delivery side. The specification of the pump is shown in Table 1.

**Table 2.1: Pump specification**

| | |
|---|---|
| Centrifugal pump | Model: GJ-10M |
| Power: 0.5 HP | Voltage: 220 V |
| Frequency: 50 Hz | Suction: 5m |
| Maximum Head: 7m | Single Impeller |

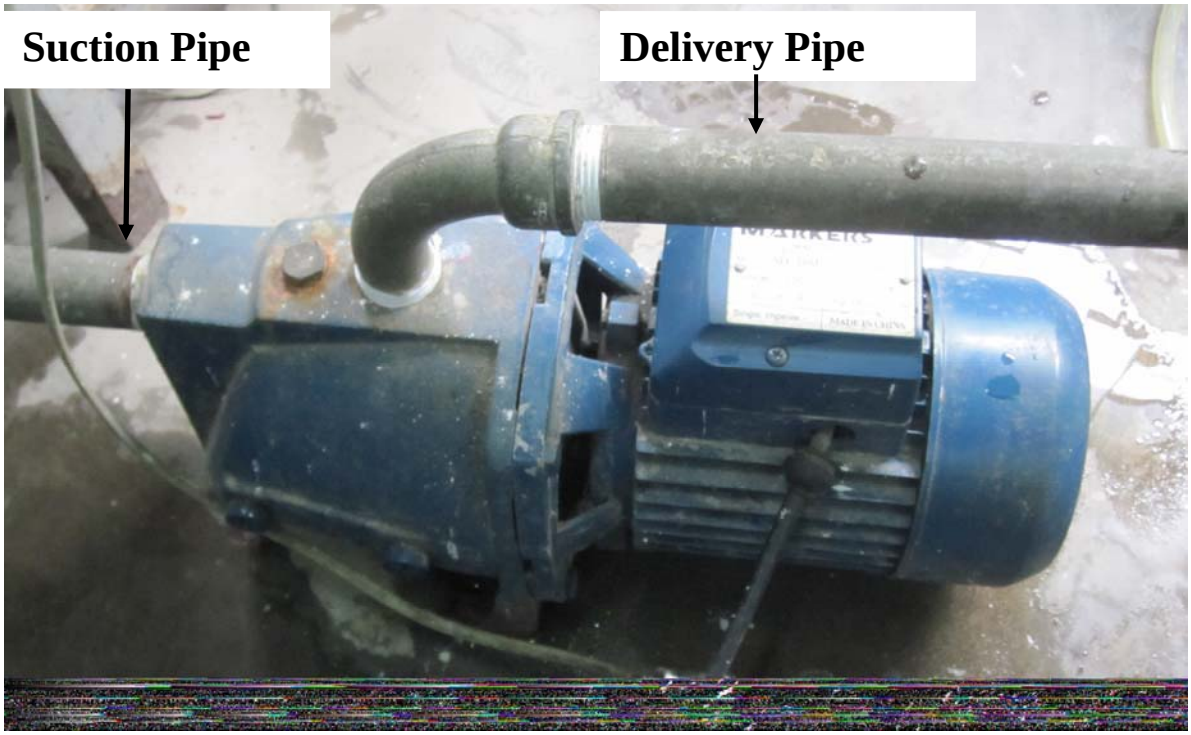


Figure 2.3: The centrifugal pump used for circulating water through the test section.

### 2.2.3: Gate Valves

Several gate valves were used for controlling and diverting the flow. The flow rate of water is controlled by the gate valve V-1 located just after the delivery of the pump. Valves V-2 and V-3 are used for diverting the flow.

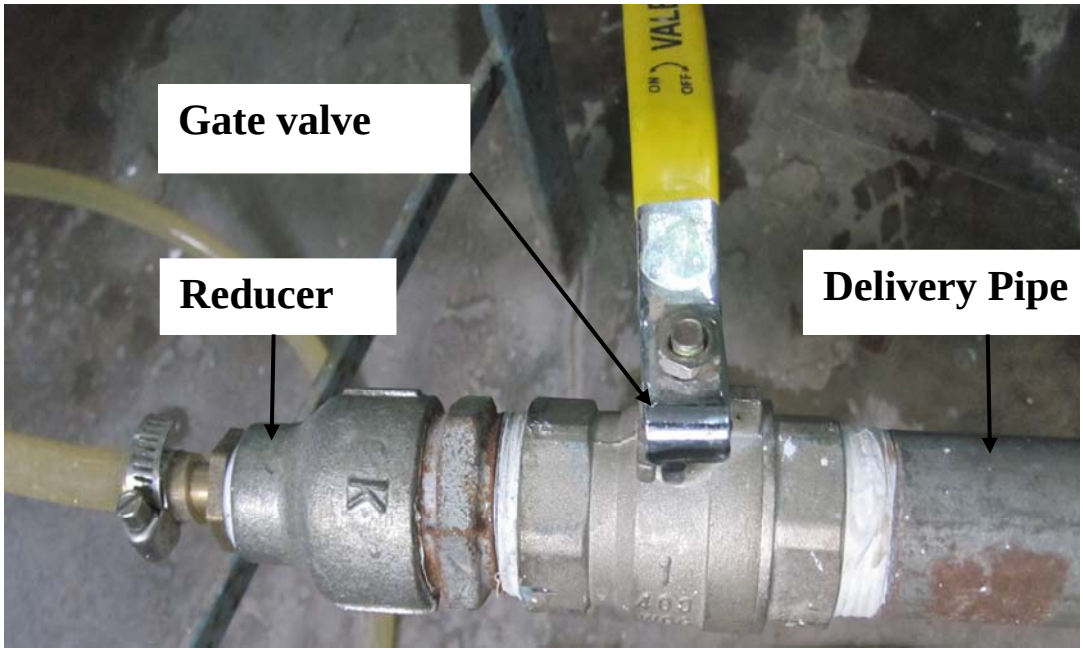


Figure 2.4: Gate valve V-1 for flow rate control.

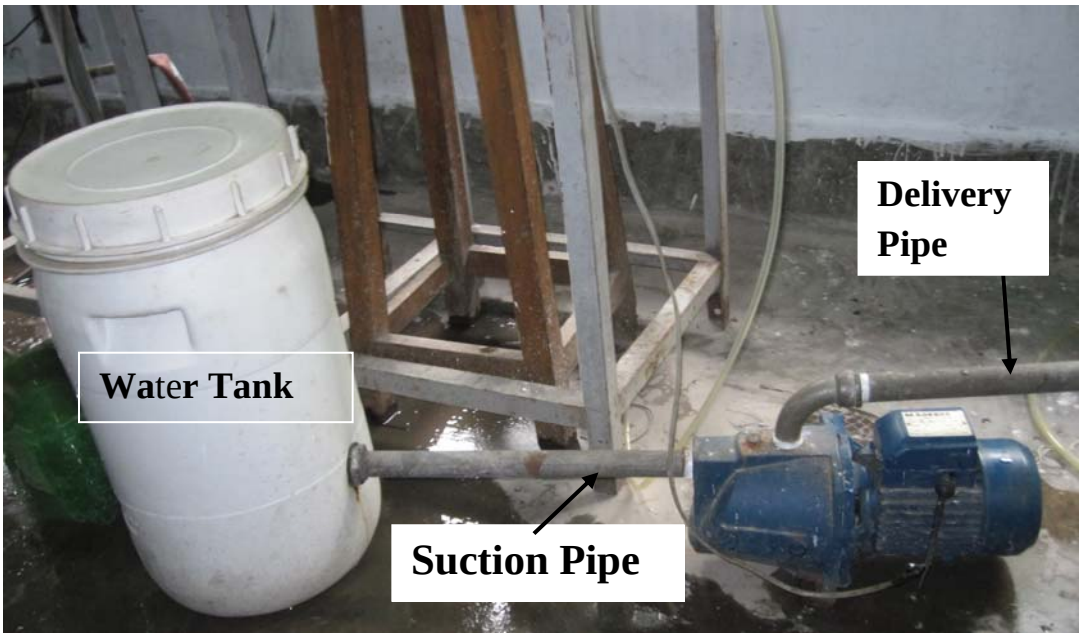


Figure 2.5 Water tank connected to the pump for supplying water to the test section.

### 2.2.4 Water Tank

A water tank is used as the reservoir of water and is connected to the suction line of the centrifugal pump. The delivery water was also discharged back into this water tank, thus forming a closed circuit system.

### 2.2.5 Measuring Flask

A 1000 cc (1 liter) measuring flask was used to measure the volume of flow. The accuracy of the measuring flask is ± 10 cc.

### 2.2.6 Wooden Frame

U-type wavy configuration of the flexible tube was made using a wooden template or frame shown in figure 2.6. It has two parts, one part is fixed to the working table and the other part is movable. Before each experimental run, the movable part was adjusted to get a desired spacer length between consecutive bends. The frame also has the facility to change the number of bends.

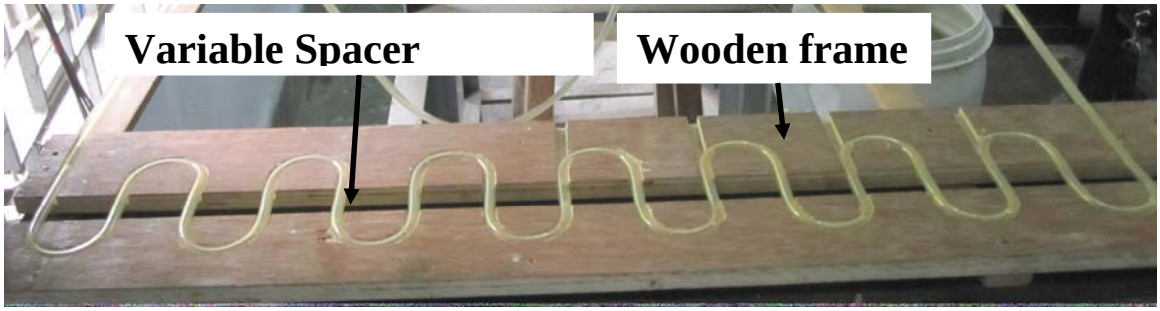


Figure 2.6 The wooden frame to form U-type wavy configuration of the flexible tube.

### 2.2.7 U-tube mercury manometer

U-tube manometer with mercury as the manometric fluid was used to measure the pressure drop. The resolution of the scale used in the manometer is 1mm. So, the uncertainty in measuring the pressure drop is ±0.5mm. The manometer is shown in Fig. 2.7. The pressure drop of the straight section is measured across the pressure tappings P-1 and P-2 to serve as a reference for the comparison of the pressure gradient between the bend and the straight tube. The total pressure drop of the straight and wavy section is measured across the pressure tappings P-1 and P-3. Valves V-2 and V-3 (see Figure 2.8) are used for switching the connection with the pressure tappings. When valve V-2 is open and V-3 is closed, the manometer measures the straight section pressure drop and when V-2 is closed and V-3 is open, it measures the total pressure drop of both the straight and the wavy sections.

Fig. 2.7 U-Tube Mercury manometer

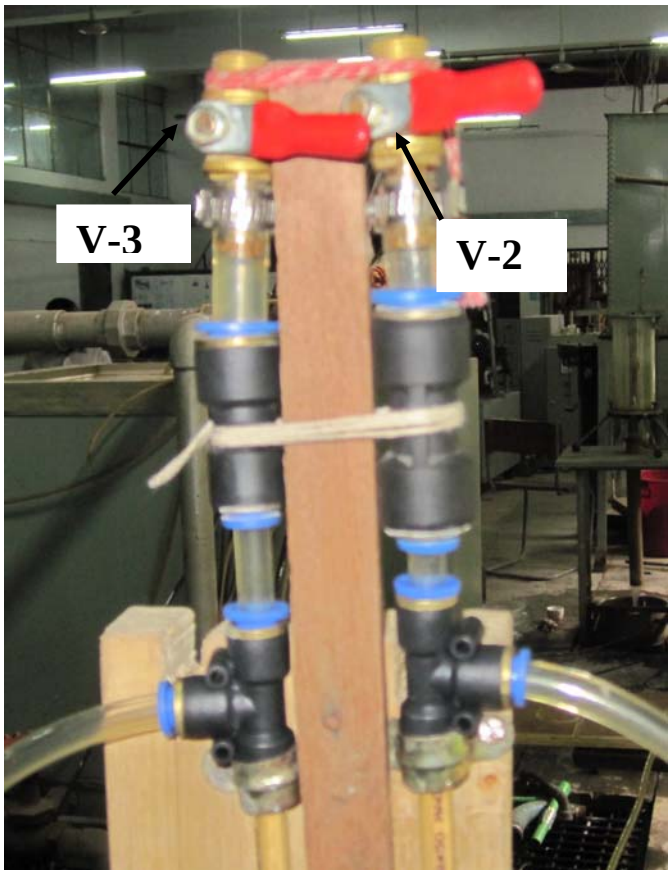


Fig. 2.8 Valves and joints at the top of the manometer (right).

### 2.2.8 Socket Reducer

A Socket Reducer shown in figure 2.9, was used for joining two tubes with different diameters. It provides leak proof joint at high pressure and changes the cross-section area of flow.

Figure-2.9: Socket Reducer.

### 2.2.9 T-joint.

T-joints as shown in figure-2.10, was used for joining three tubes with same or different diameters. It provides leak proof joint at high pressure and connects the manometer with the pressure tappings.

Figure-2.10: T- joint.

### 2.2.10 Flow control valve

Flow control valves as shown in figure 2.11 was used for controlling the flow through the tubes during measurement of pressure drop in the test section. Connection of different fittings and the flow control valve is shown in figure 2.12

Figure-2.11: Flow control valve

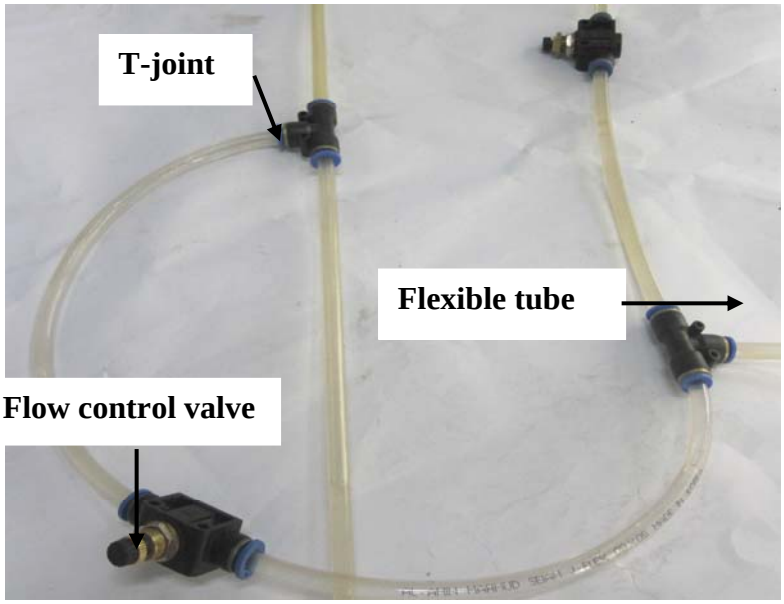


Figure 2.12 Connection of different fittings and valves with the flexible tube.

## 2.3: Experimental Procedure

Before the beginning of a run every connection was checked to see if they are connected to the proper terminals. The gate valves connected to the two sides of the mercury manometer for expelling air has to be closed before starting the pump, otherwise there will be a chance of loosing mercury through the gate valve.

The Centrifugal pump was primed first. Then it was started. Steady flow of water was supplied to the test section. Flow rate of water was controlled by a gate valve V-1 located upstream of the entrance section. The gate valve was opened slowly and the deflection of mercury in the U-tube manometer was noted. The gate valves V-2 and V-3 were both kept open. Gate valve V-4 at the top of the U-tube manometer was opened slowly to let the air trapped inside the manometer and the test section escape. Some water was also passed through the valve and the transparent flexible tube was checked to ensure no air is left inside. Gate valve V-4 was closed and in the similar way other gate valve V-5 was slowly opened and air was expelled from that side of the mercury manometer.

Then gate valve V-3 was opened and V-2 was closed so that the manometer showed the reading of total pressure drop in the system. Then the gate valve V-1 was opened slowly to get the maximum allowable flow for maximum possible pressure drop that can be measured by the manometer.

A measuring flask as shown in figure 2.13 and a stopwatch were used to measure the flow rate of water. These data were taken several times to ensure the steady flow. The manometer reading was then recorded which showed the total pressure drop of the system. Then valve V-3 was closed and valve V-2 was opened and the manometer reading was recorded which showed the value of the pressure drop in the straight section.

Flow was then reduced with the help of the delivery gate valve V-1 and corresponding pressure drops and flow rates were measured. About 20 to 30 readings were taken for each of the test section. Several data were taken for each setting to ensure that a steady flow exists in the system. The variability of the time measured for each data was kept below ± 0.1 sec. Once a reading was taken then the pump was shut down and started again to check if it gives the manometer reading within ± 0.2%.


Figure 2.13 Measurement of volume flow rate

## 2.4 Test Condition

The following conditions were ensured during the experimental runs.

a. The water level in the tank is constant in the close circuit system. The flow was, therefore, steady; that is, the flow rate did not vary with time.

b. The temperature of water was constant during each experimental run.

c. There was no air trapped inside the piping system and the manometer tubes.

d. The bends of the test section were perfectly $180^{o}$.

e. The total length of the test section 5m.

f. The material of tube is clear polyurethane.

g. There was no leakage in the system.

h. There was no deformation in the bends due to the water pressure.

i. Repeatability of measurement was ensured. Once a data was taken the pump was shut down and started again to check if it gives the manometer reading within ± 0.2%.

j. Several data were taken for each flow to ensure that a steady flow exists in the system. The variability of the time measured for each data was kept below ± 0.1 sec.

### 2.5: Uncertainty analysis

Errors are unavoidable in experiments regardless of the care which is exerted. In most of the cases the error cannot be totally eliminated even if the reason for the error is known. One can only talk about what the error might be and the limits of the possible error. The term uncertainty is used to refer to a possible value that an error may have. This section is devoted to determine the interval around which each measured parameter within which its true value is believed to lie and it will lead to the ultimate goal, that is, to estimate how great an effect the uncertainties in the individual measurements have on the calculated results. The uncertainty analysis has been carried out as described by the works of Kline and McClintock [1953, 1988]. The sample calculation is shown in Appendix-B. The maximum overall uncertainty based on Reynolds number is tabulated below.

**Table: 2.2 Uncertainty in measured values at *Re* > 20000**

| Parameter | Measured value | Uncertainty |
|---|---|---|
| $f_S$ | $6.64\times10^{-3}$ | $\pm1.74\times10^{-5}$ |
| $f_B$ | $8.38\times10^{-3}$ | $\pm 8.0\times10^{-4}$ |
| $Q$ | $7.38\times10^{-5}$ m$^3$/s | $\pm2.29\times10^{-7}$ m$^3$/s |
| $v$ | 3.760 m/s | ±0.02 m/s |
| $\Delta P_T$ | 124920.61 N/m$^2$ | ± 8.25 N/m$^2$ |
| $\rho$ | 991.25 kg/m$^3$ | ± 0.67kg/m$^3$ |
| $Re$ | 23269.85 | ±536.17 |

# Chapter 3

# RESULTS & DISCUSSION

## 3.1: Introduction

In this chapter the experimental results are presented and analyzed. Nine (09) sets of experiments are done for finding the effects of spacer length and number of bends. When experiment is done for finding the effect of a particular variable, other parameters were kept constant.

## 3.2: Parameters considered

In an experimental run, at first, the geometric parameters such as, tube or pipe diameter, radius of curvature of the bends, spacer length and number of bends are set and flow rate was varied. Flow rate and the corresponding pressure drop at the test sections were measured and recorded. Friction factors were calculated from the measured flow rate and pressure drop.

## 3.3: Data collection and calculation procedure

In each experimental run, pressure drop was measured in both straight and bend sections using mercury manometer. The locations of the pressure tapings are shown in Fig. 3.1. Time for a flow of one litter of water at various flow rates was recorded using a stop watch. Parameters such as flow rate, Reynolds number ($Re$), straight friction factor ($f_S$), bend friction factor ($f_B$) and Dean Number ($D_n$) were calculated from the recorded data.

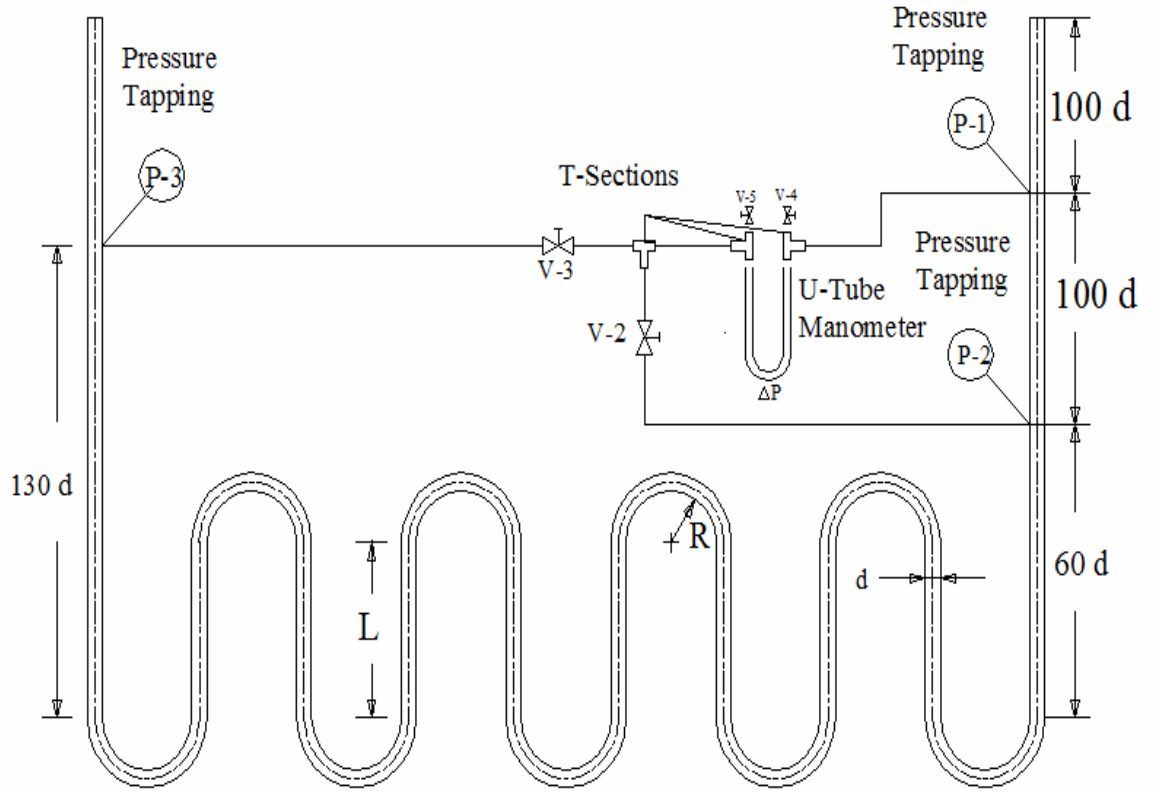


Figure 3.1: Schematic diagram of the experimental setup showing the pressure taping points.

The pressure head loss, $h_{12}$ between tapings P-1 and P-2 is calculated from the manometric deflection, $H_{12}$ using the following equitation,

$$h_{12} = H_{12}(\frac{S_g}{S_w} - 1)$$

Where, $S_g$ = Specific gravity of mercury and $S_w$ = Specific gravity of water. Experimental value of the straight friction factor, $f_s$ is calculated using Fanning formula [Lewitt, 1963].

$$f_s = \frac{2h_{12}gd}{4L_{12}v^2} \qquad 3.1$$

The Fanning friction factor is one-fourth of the Darcy friction factor and is the more commonly used by the practicing engineers and those following the British convention. It should be noted that the Darcy friction factor is defined as [White, 1999]

$$f_s = \frac{2h_{12}gd}{L_{12}v^2}$$

Where, $h_{12}$ = pressure head loss, $L_{12}$ = length of straight section between P-1 and P-2, $d$ = tube diameter and $v$ = average velocity, which is calculated from the flow rate as follows.

Flow rate, $Q = V/t$ 3.2

Where Volume, $V$ = 1 litter = 1000 cc and $t$ = time recorded by the stop watch.

Velocity, $v = Q/A$ 3.3

Where, $A$= cross sectional area of the tube. Pressure head loss between tapings P-1 and P-3 is calculated from the manometric deflection, $H_{13}$ using the following equation,

$$h_T = H_{13}(\frac{S_g}{S_w} - 1)$$

So, the pressure drop between tapings P-1 and P-3,

$$\Delta P_T = \rho g h_T \quad 3.4$$

Where, $\rho$ = density of water and $h_T$= pressure head drop between tapings P-1 and P-3.

The pressure drop in the bends may be calculated by subtracting the pressure drop in the straight section from the pressure drop in the total test section as given by equation 3.4.

Mathematically:

$$\Delta P_B = \Delta P_T - \Delta P_S \quad 3.5$$

Here, $\Delta P_S$ = Pressure drop in the straight section and the spacers between the bends, which can be calculated as,

$$\Delta P_s = \rho g \frac{4 f_S L_{st} v^2}{2gd} \quad 3.6$$

Here, $f_s$ = straight friction factor determined by equation 3.1 and $L_{st}$ = Length of straight section, $L_{12}$ + summation of the length of all spacers. If bend friction factor is $f_B$ and total

length of the curved section is $L_C$, then the bend pressure drop, i.e., the pressure drop in the curved section is given by,

$$\Delta P_B = \rho g \frac{4 L_C f_B v^2}{2gd} \qquad 3.7$$

Where total length of the curved section, $L_C = n\pi R$ for $n$ number of bends in the test section and $R$ = radius of curvature. By using equations 3.6 and 3.7, we get from equation 3.5

$$\rho g \frac{4 L_C f_B v^2}{2gd} = \Delta P_T - \rho g \frac{4 f_S L_{st} v^2}{2gd} \qquad 3.8$$

From which, on rearrangement, we get the bend friction factor,

$$f_B = \frac{\Delta P_T - \frac{4 L_{st} \rho v^2 f_s}{2d}}{\frac{4 L_c \rho v^2}{2d}} \qquad 3.9$$

Data of straight friction factor and bend friction factor are presented as a function of Reynolds number and Dean number. Reynolds number is defined as,

Reynolds number, $Re = \frac{\rho v d}{\mu}$ 3.10

Dean number is defined as, $D_n = Re\sqrt{\frac{d}{2R}}$ 3.11

Where, $\rho$ = density of water, $v$ = average velocity of water, $d$ = tube diameter and $\mu$ = absolute viscosity. The experimental data and the calculated results are listed in Table-3.1 for the case of tube diameter, $d$ = 5.00mm, radius of curvature, $R$ = 25.4mm, spacer length, $L$ = 50.8mm and number of bends, $n$ = 15. Data for all other sets of experimental run are given in appendix-A.

**Table 3.1: Experimental data and results**

Spacer Length=50.8mm, Curvature Radius=25.4mm, Number of bend=15, Straight Length=100*d*

| Pressure drop, P1 – P2 | | Pressure drop, P1 – P3 | | Full pressure | Time | Flow rate | Vel. | *Re* | $f_S$ | $f_B$ | $f_S$ (Blas.) | Dean no. |
|---|---|---|---|---|---|---|---|---|---|---|---|---|
| Right (cm) | Left (cm) | Right (cm) | Left (cm) | *(Pa)* | (Sec.) | $(m^3/s)$ | *(m/s)* | | | | | |
| 35.3 | 59.6 | -3.5 | 98 | 124920.61 | 27.09 | 7.4E-05 | 3.76 | 23370 | 0.0066 | 0.00838 | 0.0064 | 7332 |
| 37.6 | 57.6 | 1 | 94 | 114459.28 | 29.52 | 6.8E-05 | 3.45 | 21446 | 0.0065 | 0.01024 | 0.0065 | 6728 |
| 37.4 | 57.6 | 0 | 95 | 116920.77 | 30.09 | 6.6E-05 | 3.38 | 21040 | 0.0068 | 0.01098 | 0.0066 | 6601 |
| 37.8 | 57.1 | 1.5 | 93.7 | 113474.68 | 30.65 | 6.5E-05 | 3.32 | 20655 | 0.0068 | 0.01122 | 0.0066 | 6480 |
| 39 | 56 | 6.2 | 89.2 | 102151.83 | 33.1 | 6E-05 | 3.08 | 19127 | 0.0069 | 0.01202 | 0.0067 | 6001 |
| 39.5 | 55.7 | 7 | 88.2 | 99936.489 | 33.49 | 6E-05 | 3.04 | 18904 | 0.0068 | 0.01231 | 0.0067 | 5931 |
| 39.6 | 55.8 | 8 | 87 | 97228.85 | 33.76 | 5.9E-05 | 3.02 | 18753 | 0.0069 | 0.01189 | 0.0068 | 5883 |
| 40.2 | 55.1 | 11.8 | 83.8 | 88613.636 | 35 | 5.7E-05 | 2.91 | 18088 | 0.0068 | 0.01155 | 0.0068 | 5675 |
| 40.6 | 56.9 | 12 | 83 | 87382.891 | 36 | 5.6E-05 | 2.83 | 17586 | 0.0079 | 0.01086 | 0.0069 | 5517 |
| 40.1 | 55.3 | 11.7 | 84.9 | 90090.53 | 36.1 | 5.5E-05 | 2.82 | 17537 | 0.0074 | 0.01245 | 0.0069 | 5502 |
| 40.3 | 55.2 | 17 | 78 | 75075.441 | 36.7 | 5.4E-05 | 2.77 | 17250 | 0.0075 | 0.00901 | 0.0069 | 5412 |
| 41.1 | 54.4 | 13 | 82 | 84921.401 | 38.1 | 5.2E-05 | 2.67 | 16617 | 0.0072 | 0.01393 | 0.007 | 5213 |
| 41.2 | 54.3 | 16.7 | 78.7 | 76306.186 | 38.78 | 5.2E-05 | 2.62 | 16325 | 0.0073 | 0.01198 | 0.007 | 5122 |
| 41.5 | 53.9 | 19 | 77 | 71383.207 | 40.5 | 4.9E-05 | 2.51 | 15632 | 0.0076 | 0.01209 | 0.0071 | 4904 |
| 41.6 | 54 | 15.7 | 79.9 | 79013.825 | 40.7 | 4.9E-05 | 2.50 | 15555 | 0.0076 | 0.01476 | 0.0071 | 4880 |
| 42.2 | 53.4 | 21.2 | 74.4 | 65475.631 | 44.36 | 4.5E-05 | 2.29 | 14272 | 0.0082 | 0.0135 | 0.0072 | 4477 |
| 43.8 | 51.9 | 27 | 69 | 51691.288 | 49.5 | 4E-05 | 2.06 | 12790 | 0.0074 | 0.0143 | 0.0074 | 4013 |
| 43.9 | 51.9 | 27.5 | 68.6 | 50583.617 | 49.6 | 4E-05 | 2.05 | 12764 | 0.0073 | 0.01395 | 0.0074 | 4004 |
| 44 | 52 | 30 | 66 | 44306.818 | 54.4 | 3.7E-05 | 1.87 | 11638 | 0.0088 | 0.01302 | 0.0076 | 3651 |
| 44.6 | 51.5 | 31.5 | 64.5 | 40614.583 | 54.5 | 3.7E-05 | 1.87 | 11616 | 0.0076 | 0.01272 | 0.0076 | 3644 |
| 44.3 | 51.5 | 30 | 66 | 44306.818 | 56.38 | 3.5E-05 | 1.81 | 11229 | 0.0085 | 0.01544 | 0.0077 | 3523 |
| 44.5 | 51.4 | 31.5 | 64.5 | 40614.583 | 57.8 | 3.5E-05 | 1.76 | 10953 | 0.0086 | 0.0143 | 0.0077 | 3436 |
| 46 | 50 | 37.6 | 58.5 | 25722.569 | 75.27 | 2.7E-05 | 1.35 | 8411 | 0.0084 | 0.01656 | 0.0083 | 2639 |
| 46.6 | 49.5 | 40.8 | 55.3 | 17845.802 | 92 | 2.2E-05 | 1.11 | 6881 | 0.0091 | 0.01656 | 0.0087 | 2159 |
| 47.6 | 48.6 | 45.9 | 50.2 | 5292.2033 | 171 | 1.2E-05 | 0.59 | 3702 | 0.0109 | 0.01463 | 0.0101 | 1162 |

### 3.4 Verification of Experimental Data

The experimental data of straight friction factor, $f_S$ are plotted in figure 3.2 against Reynolds number ($Re$) for tube diameter, $d$ = 5 mm. The theoretical values of straight friction factor is calculated by the well known Blasius Equation given as,

$$f_s = \frac{0.0791}{(Re)^{0.25}} \qquad [4000 < Re < 10^5\ ] \qquad 3.12a$$

This friction factor known as the Fanning friction factor is one-fourth of the Darcy friction factor, which is given by [White, 1999]

$$f_s = \frac{0.316}{(Re)^{0.25}} \qquad 3.12b$$

In figure 3.2, the solid line represents the Blasius equation for turbulent flow through a hydro dynamically smooth and straight pipe. It is seen that the experimental data of straight friction factor, $f_S$ agree favorably with the predictions of the Blasius equation. This good agreement illustrates that the current experimental data are reasonably acceptable.

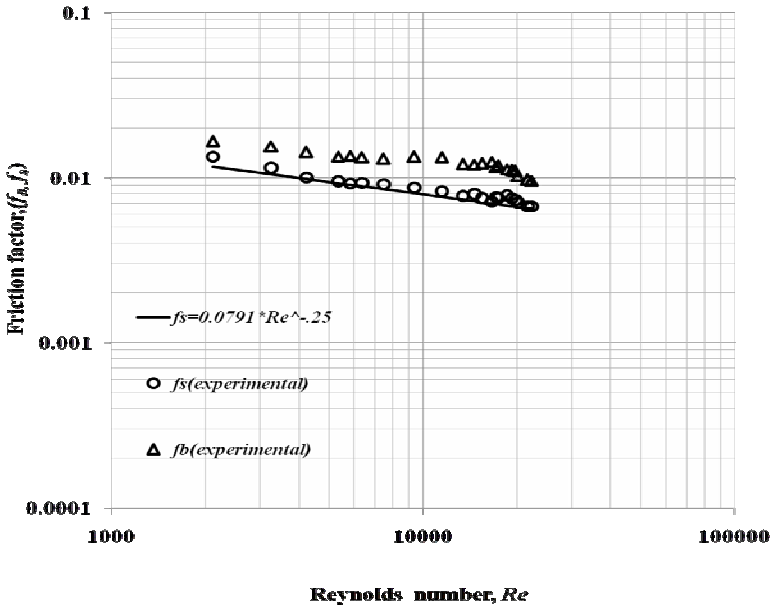


Figure 3.2 Bend friction factor, $f_B$ and straight friction factor $f_S$ vs. Reynolds number, $Re$. Experimental data and predictions by Blasius equation.

### 3.5.1: Effects of Spacer Length

In the following figures 3.3 to 3.6 bend friction factor, $f_B$ versus Reynolds number, *Re* are plotted for different spacer lengths, namely, *L = R, 2R, 3R and 4R*. Other parameters such as tube diameter, $d$ = 5.00mm, radius of curvature of the bend, $R$ = 25.4mm and number of bend, $n$ = 9 are kept in constant. From these figures we find that bend friction factor, $f_B$ decreases with increase of Reynolds numbers, *Re*.

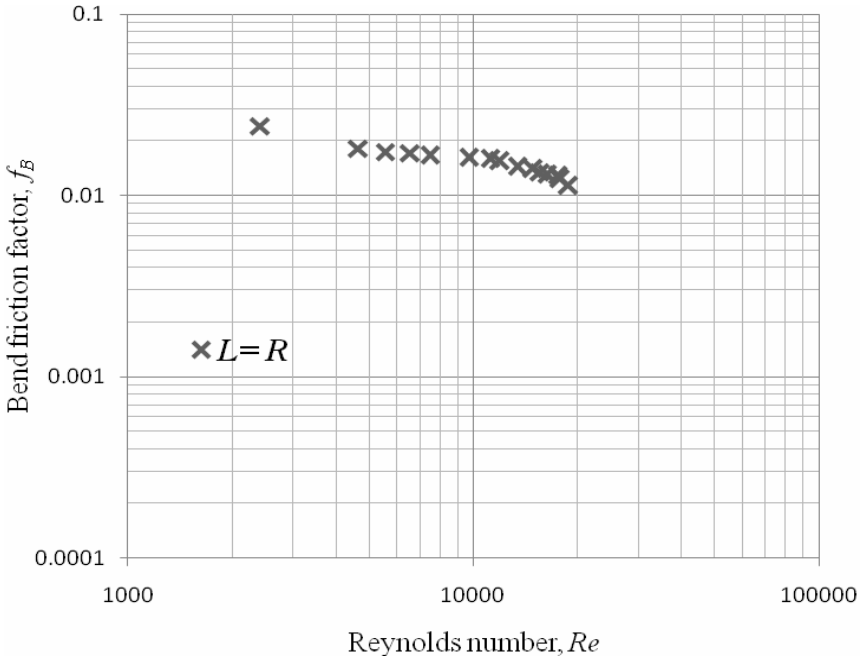


Figure-3.3: Bend friction factor ($f_B$) vs Reynolds number (*Re*) for number of bend, $n$ = 9 and spacer length, $L = R$.

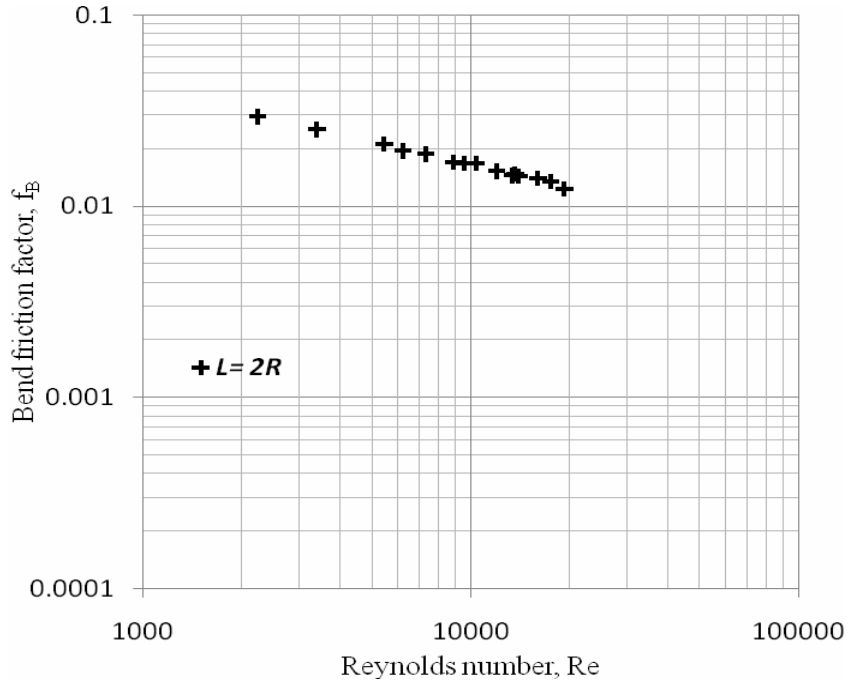


Figure- 3.4: Bend friction factor ($f_B$) *vs* Reynolds number (*Re*) for number of bend, $n = 9$ and spacer length, $L = 2R$.

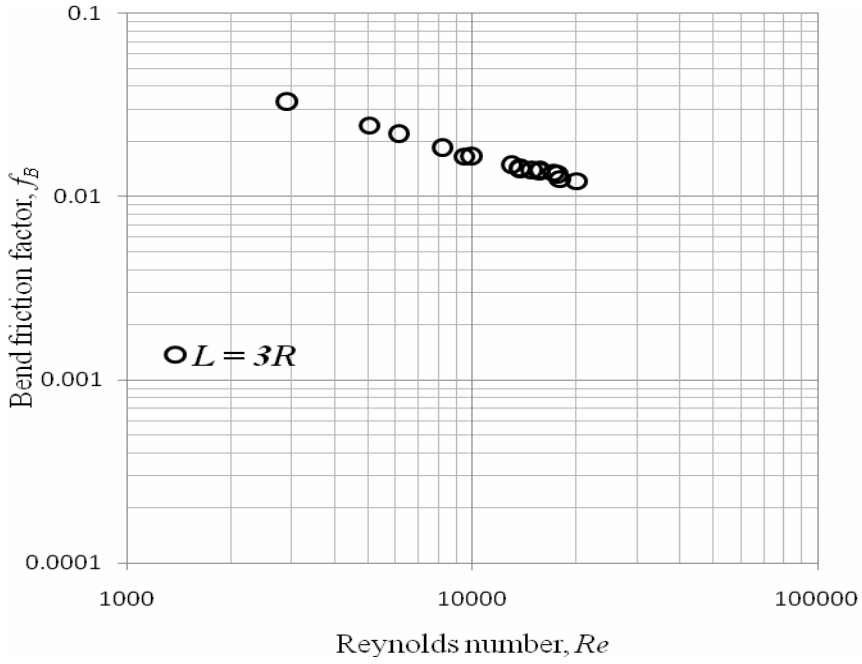


Figure- 3.5: Bend friction factor ($f_B$) *vs*. Reynolds number (*Re*) for number of bend, $n = 9$ and spacer length, $L = 3R$.

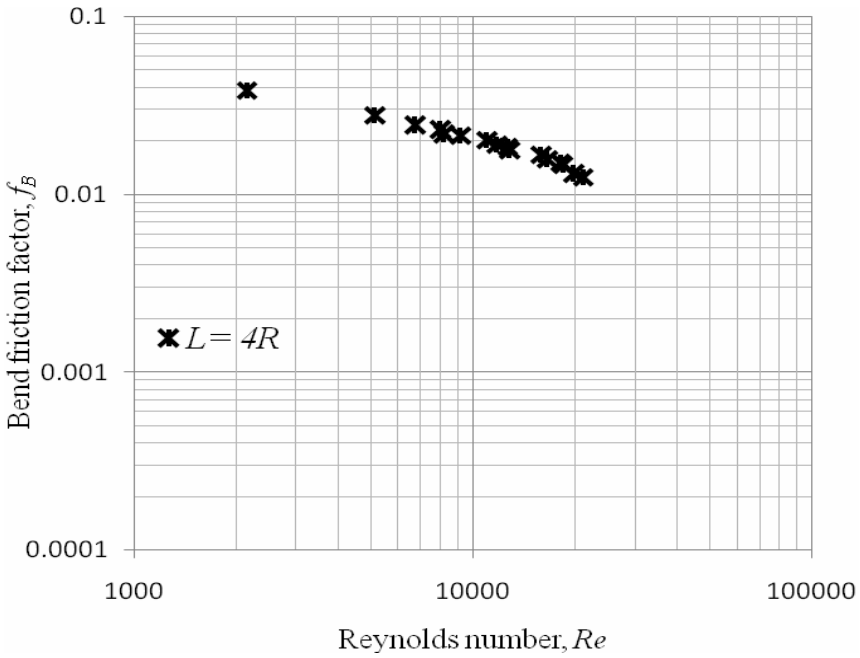


Figure- 3.6: Bend friction factor ($f_B$) *vs* Reynolds number ($Re$) for number of bend, $n = 9$ and spacer length, $L = 4R$.

The four plots in figures 3.3 to 3.6 are combined in figure-3.7 to visualize the effect of spacer length. This figure indicates that for a given Reynolds number, the bend friction factor is higher at longer spacer lengths. But the effect of spacer length seems to diminish with the increase of Reynolds number, specifically in turbulent regime.

The effect of spacer length in the turbulent regime may be visualized in a different way by plotting the bend friction factor, $f_B$ against Dean number, $D_n$ as shown in figure 3.8. This figure shows a close up view of the data points in the turbulent regime. It is evident that the effect of spacer length exists, though in a lower extent, also in the turbulent regime. However, at higher Reynolds number, in other words at higher Dean number, increase of bend friction factor with increasing spacer length diminishes.

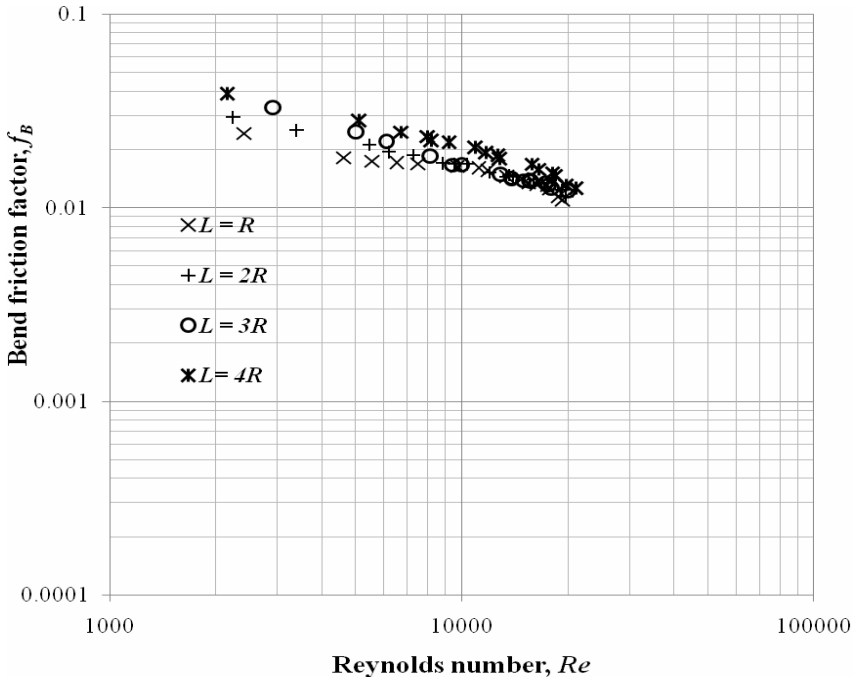


Figure- 3.7: Bend friction factor ($f_B$) *vs* Reynolds number (*Re*) for different spacer lengths.

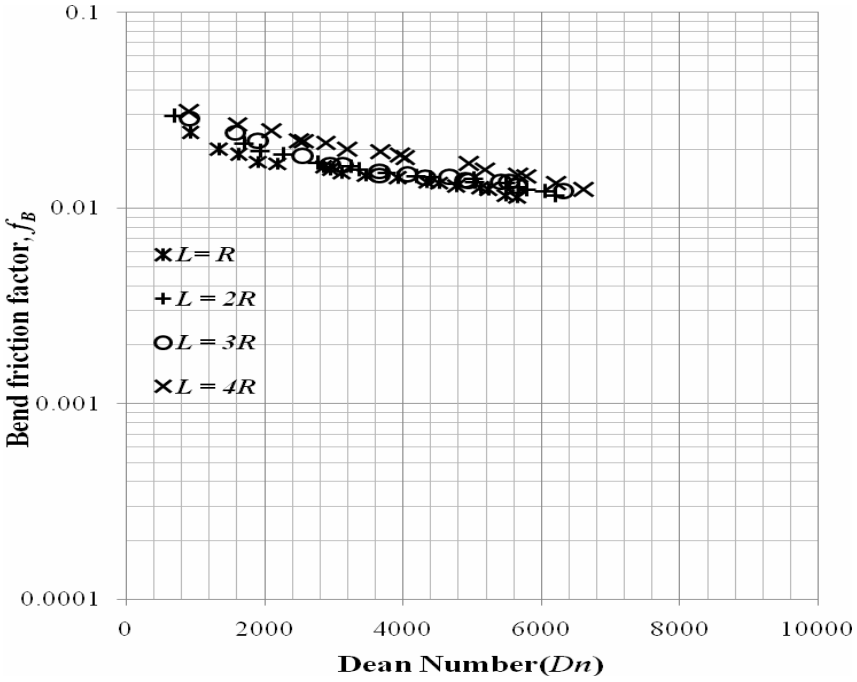


Figure 3.8: Bend friction factor, ($f_B$) *vs* Dean number, ($D_n$) for different spacer lengths.

### 3.5.2: Dimensionless Critical Spacer Length Ratio, $L_{cr}$

From the above figures 3.7 and 3.8, it is evident that with the increase of Reynolds number, bending friction factor decreases and after reaching a certain value of Reynolds number the bending friction factor, $f_B$ vs. Reynolds number, $Re$ curves for different spacer lengths overlap with each other which suggests the possibility of the existence of a dimensionless critical spacer length ratio, $L_{cr}$. The dimensionless spacer length ratio at which bend friction factor becomes independent of the number of bend is defined as critical spacer length ratio $L_{cr}$.

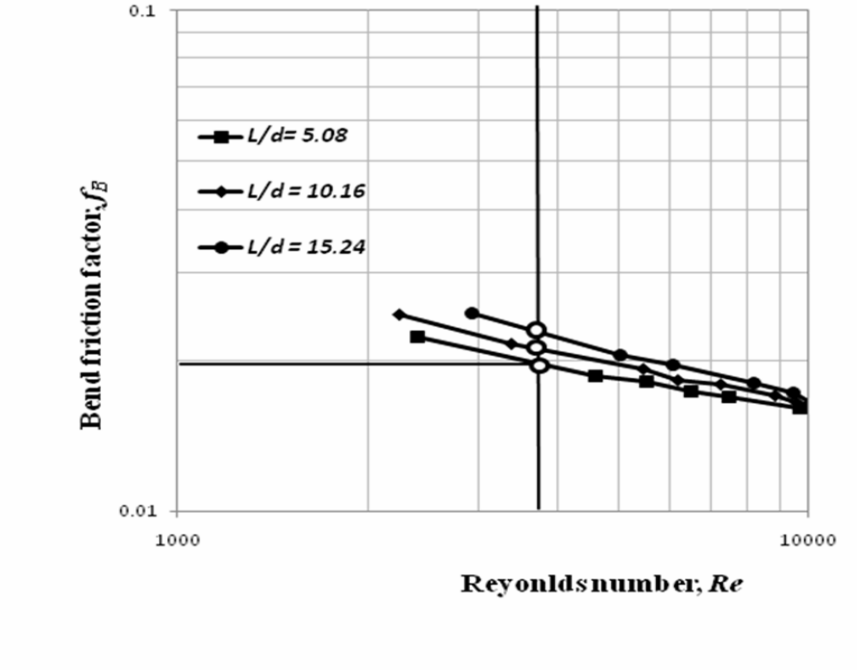


Figure- 3.9: Bend friction factor, $f_B$ *vs* Reynolds Number (*Re*) for various spacer length ratio (*L*/*d*). This plot is used for finding the friction factor at a particular Reynolds number.

In this section, the value of critical spacer length is deduced by graphical technique as shown in figure-3.9. Using figure 3.9 bend friction factor, $f_B$ is determined for various spacer lengths at a given Reynolds number. It is accomplished by drawing vertical lines for different values of Reynolds number and taking the intersecting points between the vertical line and curves as the corresponding values of the bend friction factors. Bend friction factors extracted this way

are listed in table 3.2 and are plotted against dimensionless spacer length in the figures-3.10 to 3.13.

**Table 3.2: Bend friction factors for different *L*/*d* ratio and Reynolds number (*n* = 9)**

| *L*/*d* | $f_B$ | | | |
|---|---|---|---|---|
| | *Re* = 3702 | *Re*=8000 | *Re* = 11695 | *Re* = 18088 |
| 5.08 | 0.0198201 | 0.016757 | 0.01468 | 0.012506 |
| 7.5 | 0.02094 | 0.01732 | 0.015675 | 0.012614 |
| 10.16 | 0.021853 | 0.017936 | 0.01684 | 0.013544 |
| 12.5 | 0.022015 | 0.018264 | 0.01685 | 0.01421 |
| 15.24 | 0.022335 | 0.018364 | 0.01687 | 0.0145 |
| 17.5 | 0.022357 | 0.018496 | 0.01687 | 0.01456 |
| 20.32 | 0.022388 | 0.018621 | 0.01687 | 0.014658 |

In these plots, tube diameter, $d$ = 5mm and $R$ = 25.4mm were kept constant. These figures show that for all Reynolds numbers and all spacer lengths, the value of bend friction factor ceases to increase after a certain dimensionless spacer length ratio, $L/d$ is reached.

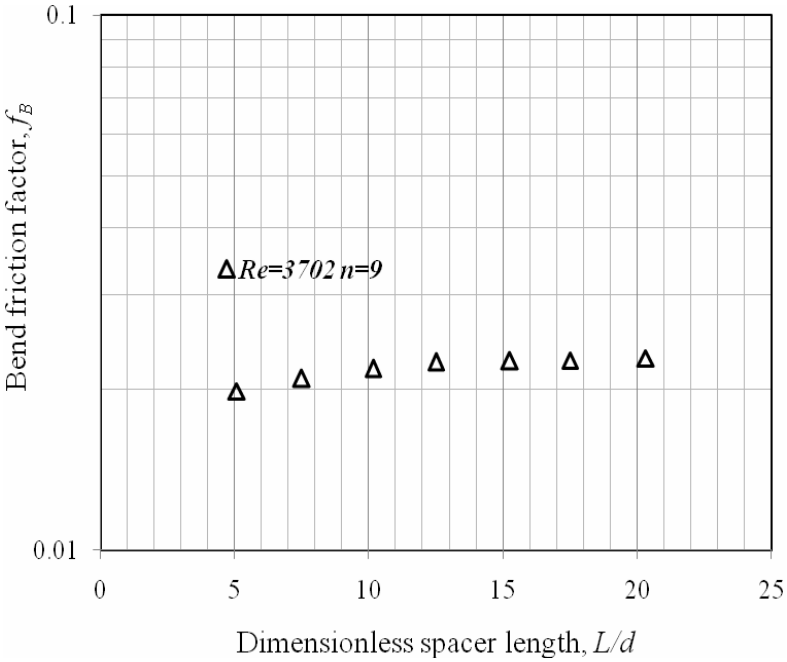


Figure 3.10 Bend friction factor, $f_B$ *vs* dimensionless spacer length for number of bend, $n$ = 9 and Reynolds number, $Re$ = 3702.

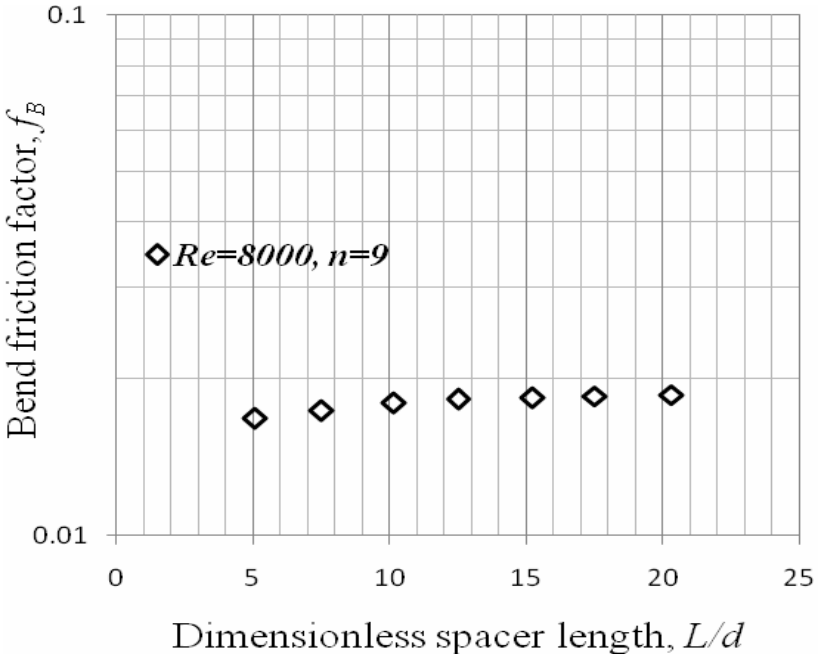


Figure 3.11: Bend friction factor, $f_B$ vs dimensionless spacer length for number of bend, $n$ = 9 and Reynolds number, $Re$ = 8000.

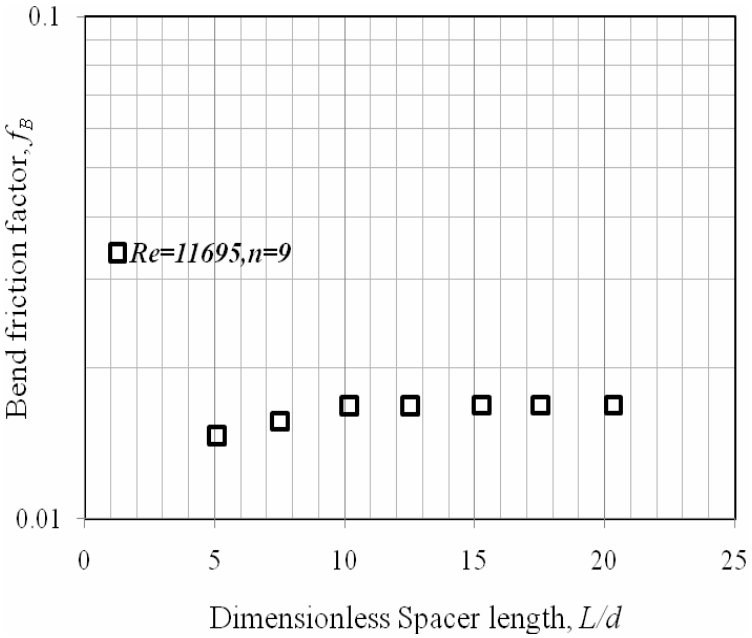


Figure 3.12: Bend friction factor, $f_B$ *vs* dimensionless spacer length for number of bend, $n$ = 9 and Reynolds number, *Re* = 11695.

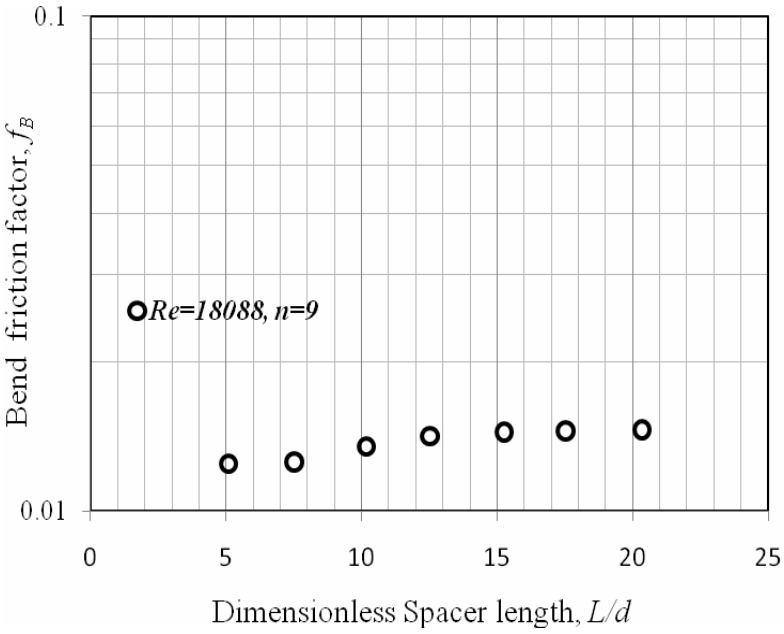


Figure 3.13: Bend friction factor, $f_B$ *vs* dimensionless spacer length for number of bend, $n$ = 9 and Reynolds number, *Re* = 18088.

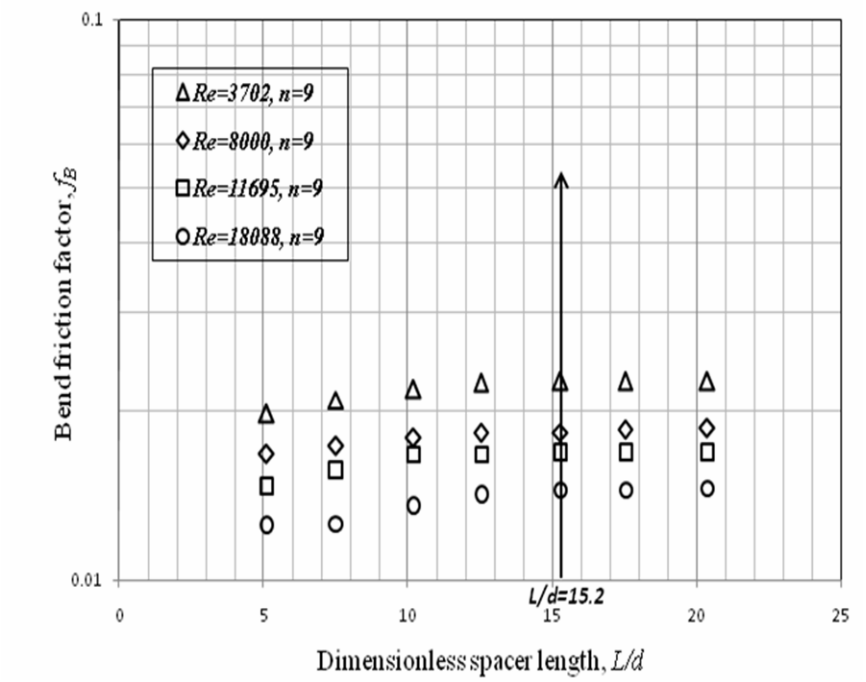


Figure 3.14: Bend friction factor, $f_B$ *vs* dimensionless spacer length.

To find the value of the dimensionless spacer length ratio after which bend friction factor does not increase with the increase of spacer length, the curves in figures 3.10 – 3.13 are combined in figure 3.14. It is evident from the figure that in all of the four cases at first the bend friction factor increases and then stop increasing at $L/d$ = 15.2 and onward. So, according to the definition it may be said that that the critical spacer length ratio, $L_{cr}$ is 15.2 in the above cases.

### 3.5.3 Effects of number of bends

The following figures 3.15 to 3.18 show the plots of bend friction factor, $f_B$ versus Reynolds number, *Re* for different number of bends, namely, $n$ = 9, 11, 13 and 15. When other parameters such as tube diameter, $d$ = 5.00mm, radius of curvature, $R$ = 25.4mm and spacer length, $L$ = 101.6mm are kept constant. From all four figures it is visible that bend friction factor decreases with increase of Reynolds number.

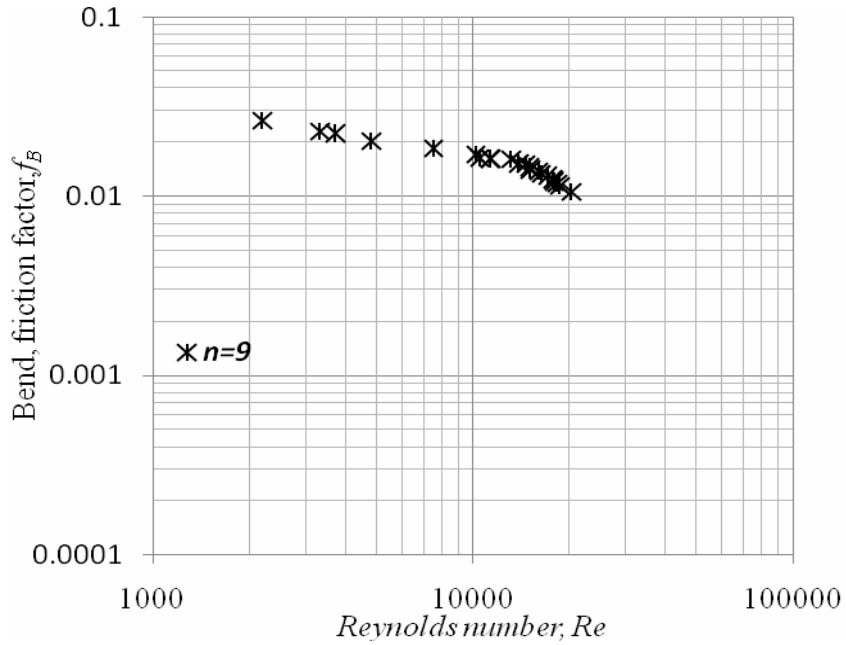


Figure 3.15: Bend friction factor, $f_B$ *vs* Reynolds number, *Re* for number of bend, $n$ = 9 and spacer length, $L = 4R$.

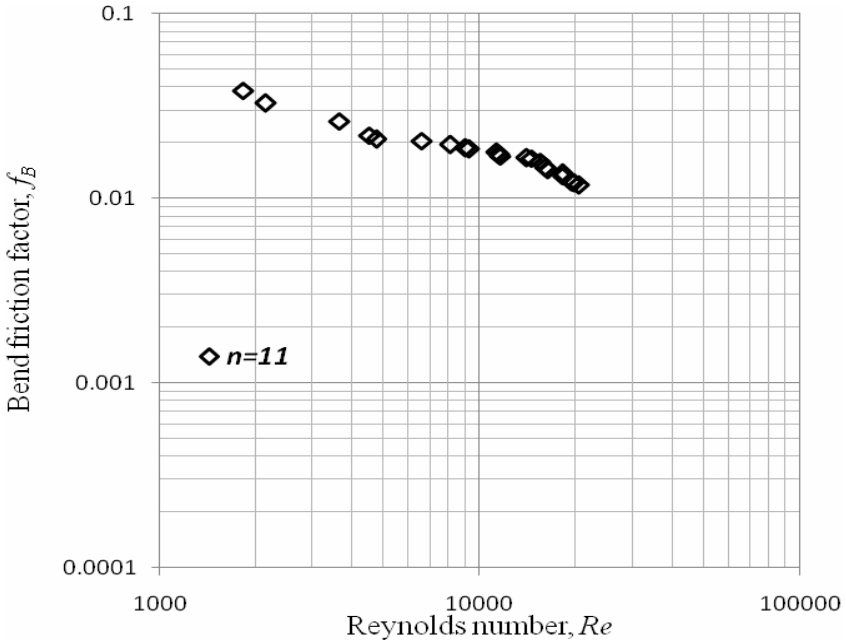


Figure 3.16: Bend friction factor, $f_B$ *vs* Reynolds number, *Re* for number of bend, $n$=11 and spacer length, $L=4R$.

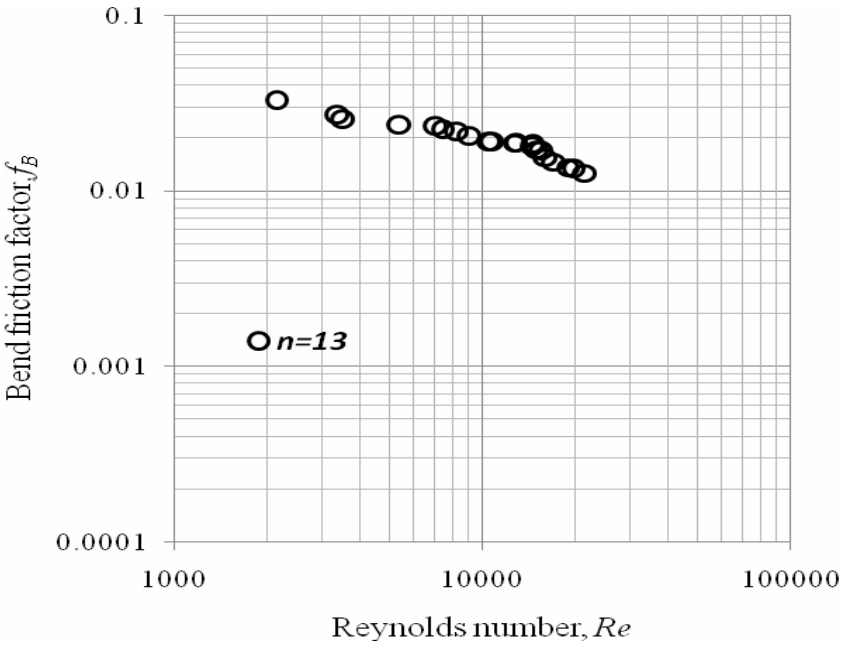


Figure 3.17: Bend friction factor, $f_B$ *vs* Reynolds number, *Re* for number of bend, *n* = 13 and spacer length, *L=4R*.

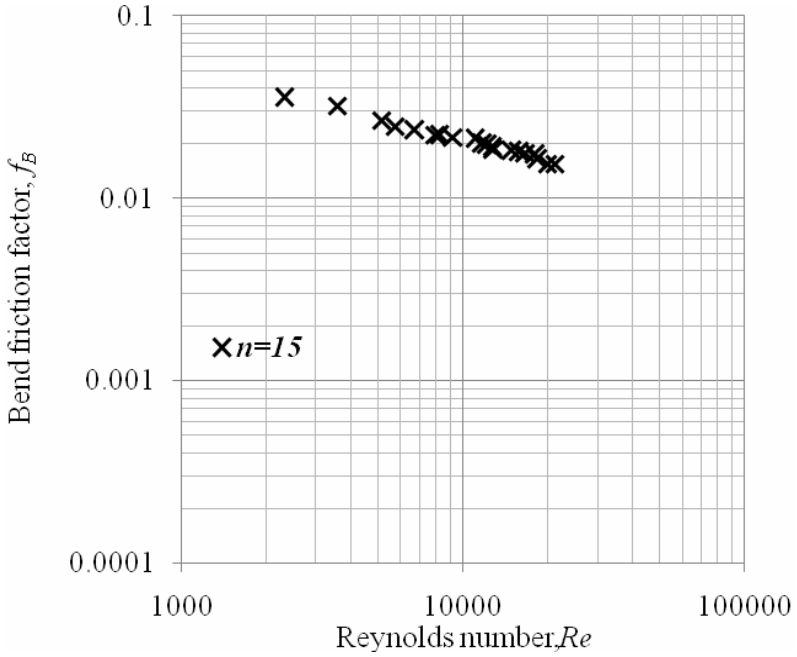


Figure 3.18: Bend friction factor, $f_B$ *vs* Reynolds number, *Re* for number of bend, *n* = 15 and spacer length, *L=4R*.

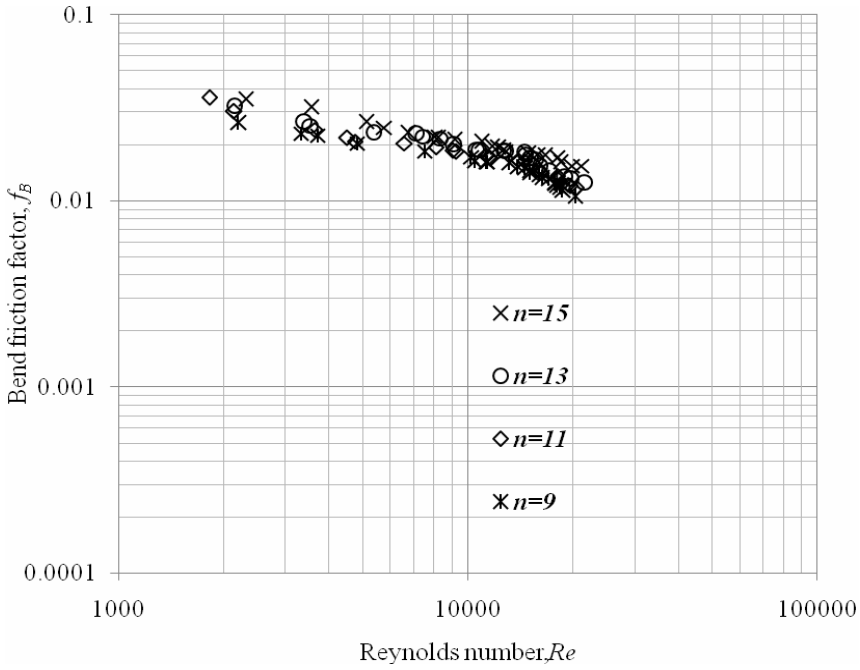


Figure 3.19: Effects of number of bends on the bend friction factor in the U-type wavy tube.

### 3.5.4 Effects of number of bends on bend friction factor and critical spacer length ratio

Figures 3.15 to 3.18 are combined in a single plot and shown in figure 3.19. From figure 3.19, it is evident that the value of bend friction factor depends on the number of bends at any Reynolds number. It is, therefore, decided to determine the value of dimensionless critical spacer length ratio at another number of bends, namely, $n$ = 15 to see whether the number of bends affects the value of the critical spacer length ratio. Following the technique shown in figure 3.9, the bend friction factor is determined from figure 3.20 for different spacer length ratio and Reynolds numbers and the values are tabulated in Table 3.3.

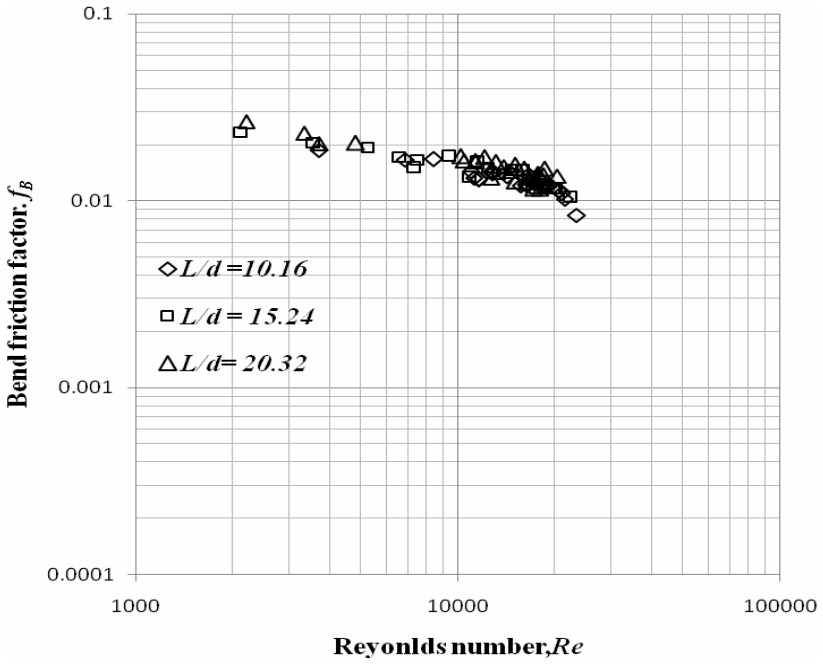


Figure 3.20: Bend friction factor, $f_B$ *vs* Reynolds Number for various spacer lengths.

**Table 3.4: Bend friction factors for different *L*/*d* ratio and Reynolds number (*n* = 15)**

| *L*/*d* | $f_B$ | | | |
|---|---|---|---|---|
| | *Re* = 3780 | *Re* = 10953 | *Re* = 12763 | *Re* = 15631 |
| 5.08 | 0.017265 | 0.013669 | 0.012053 | 0.011317 |
| 7.5 | 0.017722 | 0.013879 | 0.012242 | 0.011565 |
| 10.16 | 0.01868 | 0.01432 | 0.012639 | 0.012087 |
| 12.5 | 0.019523 | 0.015149 | 0.013386 | 0.013068 |
| 15.24 | 0.02051 | 0.01612 | 0.01426 | 0.014216 |
| 17.5 | 0.020395 | 0.016178 | 0.01442 | 0.014494 |
| 20.32 | 0.020252 | 0.01625 | 0.01462 | 0.01484 |

The values of bend friction factor, $f_B$ are plotted against dimensionless spacer length (*L*/*d*) in the figures 3.21 to 3.24 keeping other parameters such as *d* = 5mm, *R* = 25.4mm constant. Like before, these figures also show that the value of bend friction factor stops increasing and becomes stable at a dimensionless spacer length ratio, *L*/*d*.

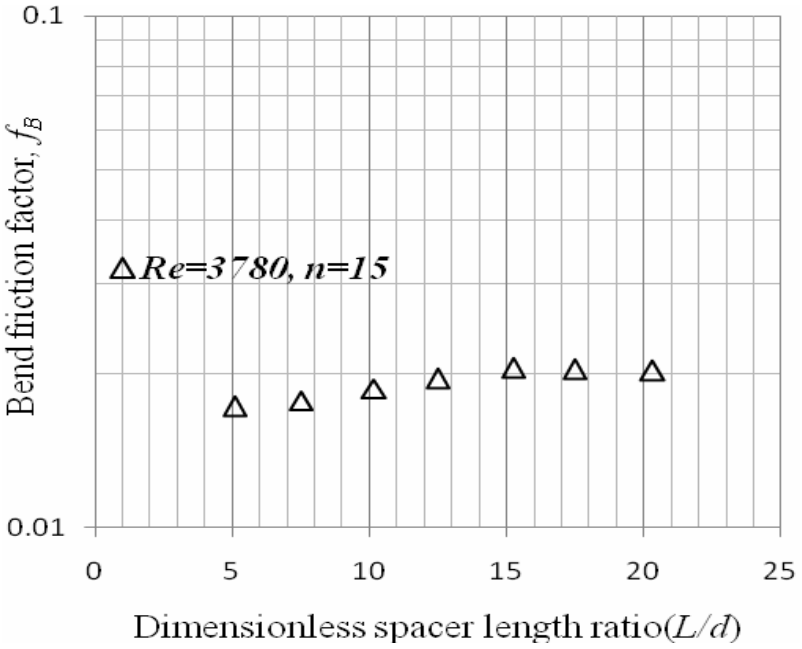


Figure 3.21: Bend friction factor, $f_B$ *vs* dimensionless spacer length, $L/d$ for number of bend, $n$ = 15 and Reynolds number, $Re$ = 3780.

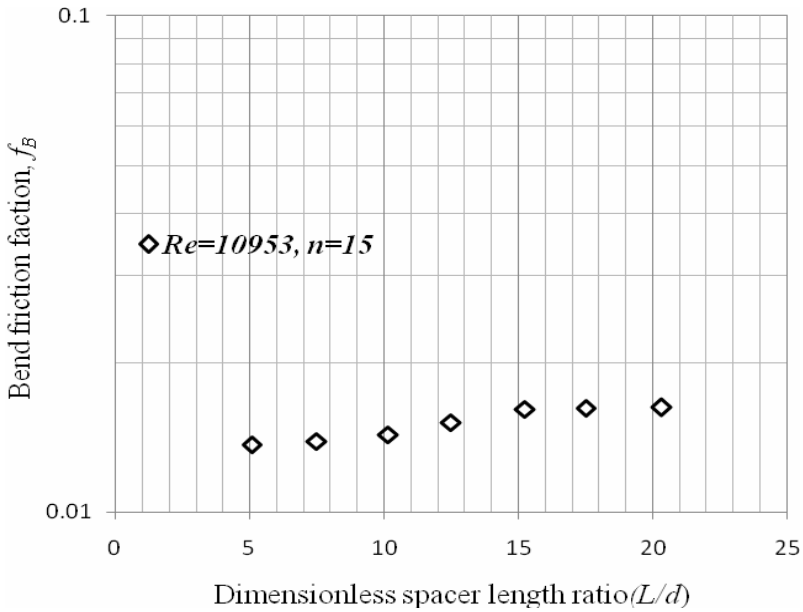


Figure 3.22: Bend friction factor, $f_B$ *vs* dimensionless spacer length $L/d$ for number of bend, $n$ = 15 and Reynolds number, $Re$ = 10953.

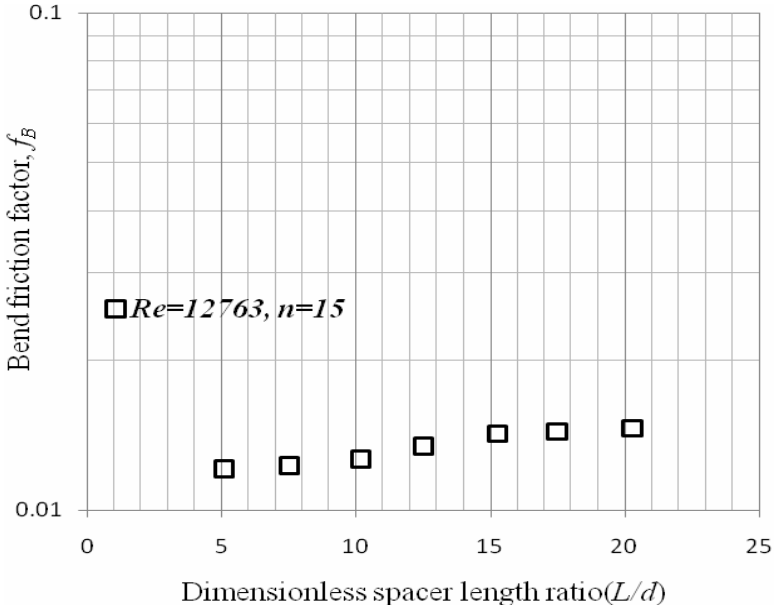


Figure 3.23: Bend friction factor, $f_B$ *vs* dimensionless spacer length $L/d$ for number of bend, $n$ = 15 and Reynolds number, $Re$ = 12763.

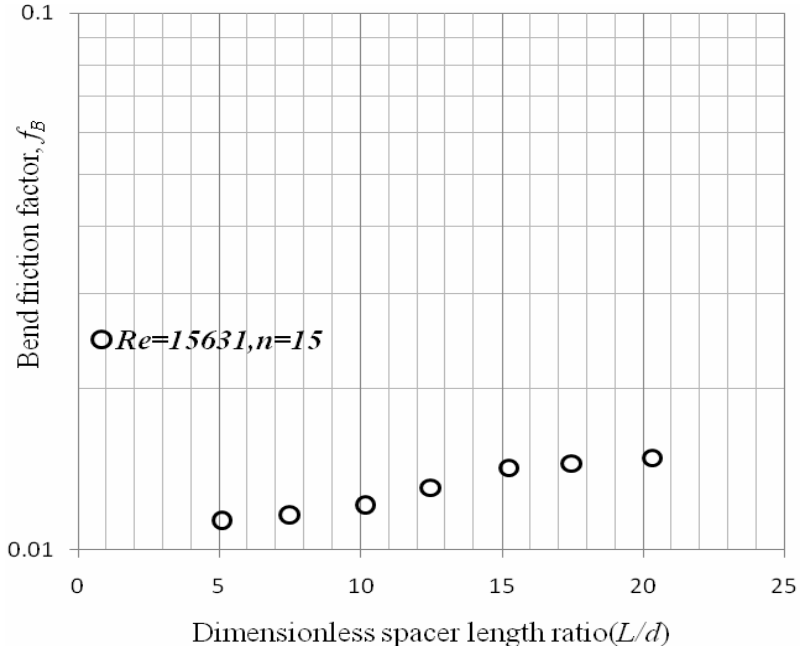


Figure 3.24: Bend friction factor, $f_B$ *vs* dimensionless spacer length $L/d$ for number of bends, $n$ = 15 and Reynolds number, $Re$ = 15631.

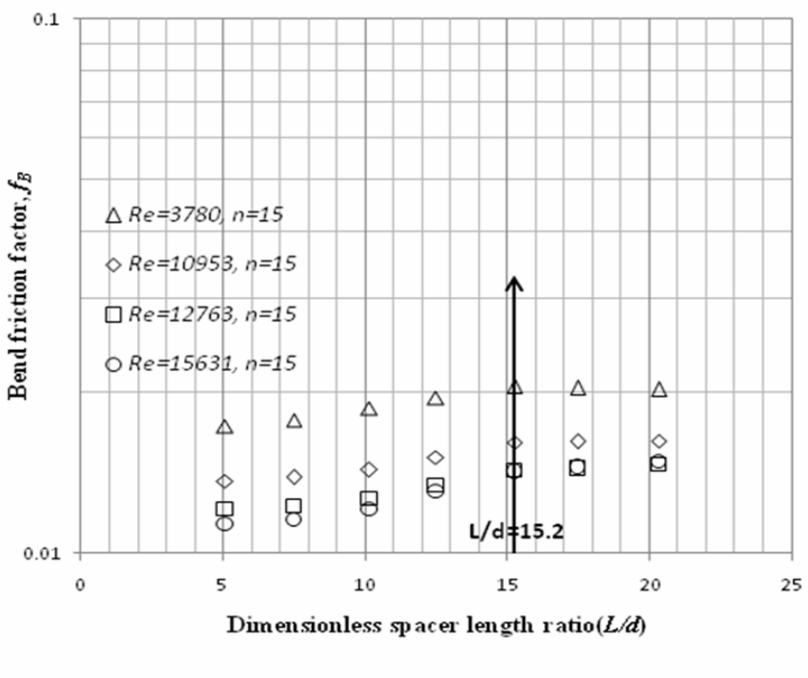


Figure 3.25: Bend friction factor, $f_B$ vs. dimensionless spacer length $L/d$ for $n$ = 15

The above figures 3.21 to 3.24 are combined in figure 3.25. It is seen that for all Reynolds number, the bend friction factor at first increases with dimensionless spacer length ratio and after reaching a value of $L/d$ of approximately equal to 15.2 stops increasing and becomes stable. This value of $L/d$ defined as the critical spacer length ratio, $L_{cr}$ is the same as that found with n = 9. As the critical spacer length ratio found from the two observations at two different numbers of bends, namely, $n$ = 9 and 15 are same, it may be concluded that there exists a critical spacer length ratio and its value is 15.2 for the present experimental condition. This value is higher than the value of the critical spacer length ratio 11.75, determined by Hanif et al. [2011] by their two dimensional CFD simulation of flow through U type wavy tubes. This means three dimensional flows need a longer spacer length to overcome the disturbances due to the presence of bends.

Figure 3.26 reproduced from Eckert's book titled Heat and Mass Transfer published by McGraw-Hill Book Company shows the effect of spacer length on heat transfer in an internal laminar flow. In this figure $x$ is the spacer length and $Nu_d$ is the Nusselt number defined as the ratio of convective to conductive heat transfer.

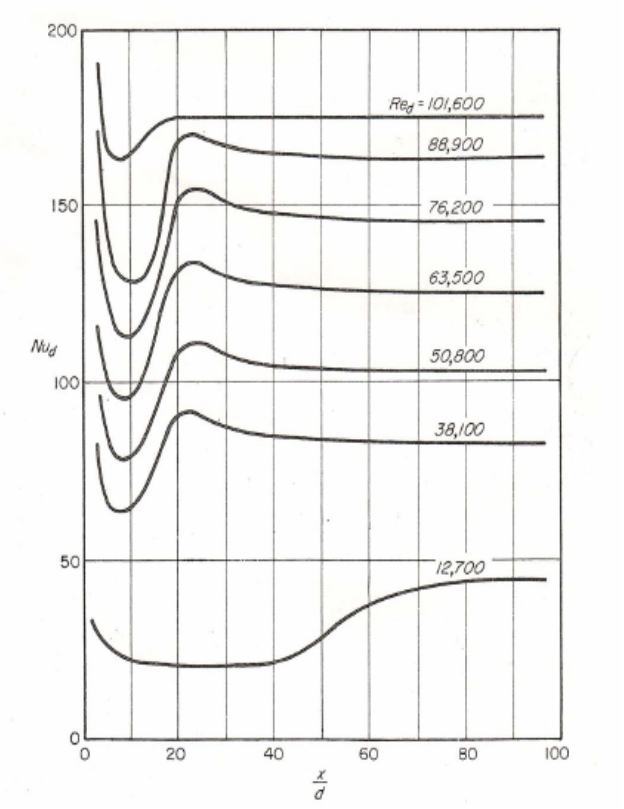


Figure 3.26: Nusselt number, $Nu_d$ vs spacer length ratio, $x/d$ for different values Reynolds number, $Re$.

From above figure, it is seen that for all Reynolds number with increase of the spacer length ratio, $x/d$, the Nusselt number, $Nu_d$ at first drops very rapidly and then rises. After reaching a value of $x/d$ of approximately equal to 30, the Nusselt number becomes almost stable. This dependence of Nusselt number on spacer length ratio implies that the mode of heat transfer also depends on spacer length. For spacer length ratio of around 10, the conductive mode of heat transfer is the most dominant mode of heat transfer. With the increase of spacer length, the influence of convective mode heat transfer increases and at a spacer length ratio of 20, the convective heat transfer is the maximum. The critical spacer length ratio 15.2 determined in the current experiment lies in between and closely corresponds to the stable values of Nusselt number which implies that a balance between convective and conductive modes of heat transfer is obtained at this critical spacer length ratio.

# Chapter 4

# CONCLUSION

## 4.1 Major Outcomes

In this work an experimental set-up for measuring pressure drop and friction factor in U-type wavy tubes is designed and fabricated. Pressure drops have been measured in U-type wavy tubes of different number bends and spacer lengths and friction factors have been calculated. In the experiment, Reynolds number was ranged between 1000 and 23500 and Dean number was varied from 500 to 7000. The results may be summarized as follows.

- It has been found that the bend friction factor, $f_B$ decreases with the increase of Reynolds Numbers, *Re*.
- At large values of Reynolds number, the differences in bend friction factors due to variations in spacer lengths or number of bends diminishes.
- The bend friction factor, $f_B$ increases with the increase of the spacer length up to the critical spacer length ratio.
- The dimensionless critical spacer length ratio is found to be 15.2. This value of critical spacer length ratio is not affected by the number of bends.
- The critical spacer length ratio corresponds to a balance between convective and conductive modes of heat transfer in a U-type wavy tube.

These findings will be useful in designing fluid flow through U-type wavy tubes in various kinds of heat transfer equipment.

## 4.2 Scope for Future Work

- In this work, experiment has been performed using only water as the working fluid. Further investigation may be done with air and other liquids and even with multiphase flow.
- A critical spacer length has been identified for U-type wavy tubes. Investigation may be done to determine the critical curvature ratio, beyond which the curvature of the pipe may be neglected.
- A general design correlation may be developed considering the critical spacer length ratio and critical curvature ratio which will be very useful in designing flow through U-type wavy tubes in various appliances.

# REFERENCES

Aland S., Weydahl, E., Siegel, J. M. and Moore, J., 1998, “Computational analysis of flow in a curved tube model of the coronary arteries: effects of time-varying curvature”, Annals of Biomedical Engineering, Vol. 26, pp. 944–954.

Chen, I. Y., Lai, Y. K. and Wang, C. C., 2003, “Frictional performance of U-type wavy tubes”, ASME J. Fluids Engg., 125, pp. 880-886.

Chen, I. Y., Wang, C. C. and Lin, S. Y., 2004, “Measurements and correlations of frictional single-phase and two-phase pressure drops of R-410A flow in small U-type return bends”, Int. J. Heat Mass Trans. 47, 10-11, pp. 2241–2249.

Chen, I.Y., Won, C. L. and Wang, C.C., 2005, “Influence of oil on R-410A two-phase frictional pressure drop in a small U-type wavy tube”, Int. Commun. in Heat and Mass Transfer, 32, 6, Pp. 797–808.

Chen, I. Y., Wu, Y. S., Liaw, J. S. and Wang, C. C., 2008, “Two-phase frictional pressure drop measurements in U-type wavy tubes subject to horizontal and vertical arrangements”, J. Applied Thermal Engineering, 28, 8-9, Pp. 847–855.

Chen, I. Y., Yang, K. S., and Wang, C. C., 2001, “Two-phase frictional pressure drop of air-water in small horizontal tubes”, J. Thermophys. Heat Transfer, 15, 4, pp. 409–415.

Chen, I. Y., Yang, Y. W., and Wang, C. C., 2002, “Influence of horizontal return bend on the two-phase flow pattern in a 6.9-mm diameter tube”, Can. J. Chem. Eng., 80, 3, pp. 478–484.

Cho, K. and Tae, S. J., 2001, “Condensation heat transfer for R-22 and R-407 refrigerant oil mixtures in a microfin tube with a U-bend”, Int. J. Heat Mass Transfer, 44, 11, pp. 2043-2051

Ciofalo, M. and Piazza, I. D., 2000, “Investigation of flow and heat transfer in corrugated-undulated plate heat exchangers”, J. Heat and Mass Transfer, Springer

Das, K., Alam, M. M. and Razzaque, M. M., 2007, “Turbulent regime friction factors for U-type wavy tubes”, Paper no: ICME07-FL23, ICME, Dhaka, Bangladesh.

Domanski, P. A. and Hermes, C. J. L., 2008, “An improved correlation for two-phase pressure drop of R-22 and R-410a in 180° return bends”, J. Appl. Thermal Engg., 28, 7, pp. 793–800.

Eckert, E. R. G., Heat and Mass Transfer, McGraw-Hill, Inc.

Hamim, S. A., Khan, A. and Razzaque, M. M., 2008, “Prediction of friction factors for U-type wavy tubes”, The 4$^{th}$ BSME-ASME Int. Conf. on Thermal Engg., Dhaka, Bangladesh, Paper no:133, pp. 350-355.

Hanif, S. E. A., Hossain, S. and Razzaque, M. M., 2011, “Effect of curvature ratio and spacer length ratio on the U-type wavy tube by CFD analysis”, International Conference on Mechanical, Automotive and Aerospace Engineering (ICMAAE), Kualalampur, Malaysia.

Huzarewicz, S. and Gupta, R. K. 1991, “Elastic effects in flow of fluids through sinuous tubes”, Journal of rheology.

Ito, H., 1960, “Pressure losses in smooth pipe bends”, ASME J. Basic Engg., 82 pp. 131-143.

James, D.F., Thien, N. P., Khan, M. M. K., Beris, A. N. and Pilitsis, S., 1990, “Flow of test fluid M1 in corrugated tubes”, Journal of Non-Newtonian Fluid Mechanics, 35, 2-3, Pp. 405–412.

Lewitt, E. H., 1963, Hydraulics and Fluid Mechanics, Tenth Edition, The English Language Book Society.

Lynch, D. G., Waters, S. L. and Pedley, T. J., 1996, “Flow in a tube with non-uniform, time-dependent curvature: governing equations and simple examples” J. Fluid Mechanics, 323 : pp 237-265.

Manlapaz, R. L., and Churchill, S. W., 1980, “Fully developed laminar flow in a helical coiled tube of finite pitch“, Chem. Commun. Cambridge, 7, pp. 57–58.

Popiel, C. O., and van der Merwe, D. F., 1996, “Friction factor in sine-pipe flow, ASME J. Fluids Engg., 118, pp. 341–345.

Popiel, C. O. and Wojtkowiak, J., 2000, “Friction factor in U-type undulated pipe flow”, ASME J. Fluids Engg., 122, pp. 260-263.

Potter, M. C. and Wiggert, D. C., 1991, Mechanics of Fluds, Prenice Hall, Inc.

Razzaque, M. M., Hanif, S. E. A. and Hossain, S., 2010, “Effect of spacer length between consecutive bends on friction factors of U-type wavy tubes: CFD analysis”, The 13th Asian Congress of Fluid Mechanics, 17-21 December, Dhaka, Bangladesh.

Reno, F., Leuliet, J. C. and Delplace, F., 1993, “Friction factors and roughness measurements of tubular mineral membranes”, Food Process Engineering Lab., INRA, 369.

Rogers, G. F. C. and Mayhew, Y.R., 1964, “Heat transfer and pressure loss in helically coiled tubes with turbulent flow”, International Journal of Heat and Mass Transfer, 7, 11, Pp.1207-1216.

Shames, I. H., 1992, Mechanics of fluids, International Edition, McGraw-Hill, Inc.

Sivashanmugam, P. and Suresh, S., 2006, “Experimental studies on heat transfer and friction factor characteristics of laminar flow through a circular tube fitted with helical screw-tape inserts”, J. Applied Thermal Engineering, 26, 16, Pp. 1990–1997.

Shimizu, Y., Sugino, K., Kuzuhara, S., and Murakami, M., 1982, “Hydraulic losses and flow patterns in bent pipes – comparison of the results in wavy pipes and quasi-coiled ones”, Bul. JSME, 25, pp. 24–31.

Von Bernuth, R. D., and Wilson, T., 1989, “Friction factors for small diameter plastic pipes”, J. Hydraul. Eng., 115(2), pp.183–192.

Wang, C. C., Chen, I. Y. and Shyu, H. J., 2003, “Frictional performance of R-22 and R-410a inside a 5.0 mm diameter wavy tube”, Int. J. Heat Mass Trans. 46, 4, pp. 755–760.

Ward-Smith, A. J., 1980, The Fluid Dynamics of Flow in Pipes and Ducts. Chapter B: Bends, Clarendon Press, Oxford, pp. 248–306.

White, F. M., 1999, “Fluid Mechanics”, Fourth edition., McGraw-Hill Inc.

Wojtkowiak, J. and Popiel, C. O., 2000, “Effect of cooling on pressure losses in U-type wavy pipe flow”, Int. Commun. Heat Mass Trans. 27, 2, pp. 169-177.

Yutasak, C. and Somchai, W., 2005, “Effect of fin pattern on the air-side of herringbone wavy fin-and-tube heat exchangers”, J. Heat Mass Transfer, 41, pp. 642-650.

# Appendix-A

# Experimental data and results

## Table A.1 Experimental data for Spacer Length=2R, Curvature Radius=25.4mm, Number of bend=15

| Straight pressure reading | | Full pressure reading. | | Total pressure | Time | Flow rate | Velocity | Reynolds | | | Dean |
|---|---|---|---|---|---|---|---|---|---|---|---|
| Right(cm) | left(cm) | Right (cm) | Left (cm) | $N/m^2$(Pa) | (Sec.) | ($m^3$/sec) | (m/sec) | no. *Re* | $f_S$ | $f_B$ | no. |
| 35.3 | 59.6 | -3.5 | 98 | 124920.61 | 27.09 | 7.3828E-05 | 3.760019 | 23369.85 | 0.0066392 | 0.008377 | 7331.77 |
| 37.6 | 57.6 | 1 | 94 | 114459.28 | 29.52 | 6.77507E-05 | 3.450505 | 21446.12 | 0.0064886 | 0.010238 | 6728.24 |
| 37.4 | 57.6 | 0 | 95 | 116920.77 | 30.09 | 6.64673E-05 | 3.385142 | 21039.86 | 0.0068091 | 0.010985 | 6600.79 |
| 37.8 | 57.1 | 1.5 | 93.7 | 113474.68 | 30.65 | 6.52529E-05 | 3.323292 | 20655.44 | 0.0067501 | 0.011225 | 6480.19 |
| 39 | 56 | 6.2 | 89.2 | 102151.83 | 33.1 | 6.0423E-05 | 3.077308 | 19126.57 | 0.0069342 | 0.012018 | 6000.53 |
| 39.5 | 55.7 | 7 | 88.2 | 99936.489 | 33.49 | 5.97193E-05 | 3.041472 | 18903.83 | 0.0067645 | 0.012312 | 5930.66 |
| 39.6 | 55.8 | 8 | 87 | 97228.85 | 33.76 | 5.92417E-05 | 3.017148 | 18752.65 | 0.006874 | 0.011887 | 5883.22 |
| 40.2 | 55.1 | 11.8 | 83.8 | 88613.636 | 35 | 5.71429E-05 | 2.910255 | 18088.27 | 0.0067954 | 0.01155 | 5674.79 |
| 40.6 | 56.9 | 12 | 83 | 87382.891 | 36 | 5.55556E-05 | 2.829414 | 17585.81 | 0.0078647 | 0.010863 | 5517.16 |
| 40.1 | 55.3 | 11.7 | 84.9 | 90090.53 | 36.1 | 5.54017E-05 | 2.821576 | 17537.10 | 0.0073748 | 0.012454 | 5501.87 |
| 40.3 | 55.2 | 17 | 78 | 75075.441 | 36.7 | 5.44959E-05 | 2.775447 | 17250.39 | 0.0074715 | 0.009013 | 5411.93 |
| 41.1 | 54.4 | 13 | 82 | 84921.401 | 38.1 | 5.24934E-05 | 2.673462 | 16616.52 | 0.0071878 | 0.013926 | 5213.06 |
| 41.2 | 54.3 | 16.7 | 78.7 | 76306.186 | 38.78 | 5.1573E-05 | 2.626583 | 16325.15 | 0.0073346 | 0.011979 | 5121.65 |
| 41.5 | 53.9 | 19 | 77 | 71383.207 | 40.5 | 4.93827E-05 | 2.515035 | 15631.83 | 0.0075722 | 0.012087 | 4904.14 |
| 41.6 | 54 | 15.7 | 79.9 | 79013.825 | 40.7 | 4.914E-05 | 2.502676 | 15555.02 | 0.0076472 | 0.014762 | 4880.04 |
| 42.2 | 53.4 | 21.2 | 74.4 | 65475.631 | 44.36 | 4.50857E-05 | 2.296188 | 14271.62 | 0.0082053 | 0.013495 | 4477.40 |
| 43.8 | 51.9 | 27 | 69 | 51691.288 | 49.5 | 4.0404E-05 | 2.057756 | 12789.68 | 0.007389 | 0.014302 | 4012.48 |
| 43.9 | 51.9 | 27.5 | 68.6 | 50583.617 | 49.6 | 4.03226E-05 | 2.053607 | 12763.9 | 0.0073273 | 0.013949 | 4004.39 |
| 44 | 52 | 30 | 66 | 44306.818 | 54.4 | 3.67647E-05 | 1.872406 | 11637.67 | 0.0088141 | 0.013024 | 3651.06 |
| 44.6 | 51.5 | 31.5 | 64.5 | 40614.583 | 54.5 | 3.66972E-05 | 1.868971 | 11616.32 | 0.0076302 | 0.012716 | 3644.36 |
| 44.3 | 51.5 | 30 | 66 | 44306.818 | 56.38 | 3.54736E-05 | 1.80665 | 11228.97 | 0.0085207 | 0.015438 | 3522.84 |
| 44.5 | 51.4 | 31.5 | 64.5 | 40614.583 | 57.8 | 3.46021E-05 | 1.762265 | 10953.10 | 0.0085822 | 0.014302 | 3436.29 |
| 46 | 50 | 37.6 | 58.5 | 25722.569 | 75.27 | 2.6571E-05 | 1.353247 | 8410.913 | 0.0084371 | 0.016555 | 2638.73 |
| 46.6 | 49.5 | 40.8 | 55.3 | 17845.802 | 92 | 2.17391E-05 | 1.107162 | 6881.407 | 0.0091383 | 0.016557 | 2158.88 |

**Table A.2 Experimental data for Spacer Length=3R, Curvature Radius=25.4mm, Number of bend=15**

| Straight pressure reading | | Full pressure reading. | | Total pressure | Time(Sec.) | Flow rate | Velocity | | $f_S$ | $f_B$ | Dean no. |
|---|---|---|---|---|---|---|---|---|---|---|---|
| Right(cm) | left(cm) | right(cm) | left(cm) | $N/m^2$(Pa) | | $m^3/sec$ | m/sec | Reynolds no. *Re* | | | |
| 36.3 | 58.5 | -4 | 99 | 126766.7 | 28.5 | 7.0175E-05 | 3.573997 | 22213.67 | 0.006713 | 0.010546 | 6969.047 |
| 37.9 | 57 | 2 | 93 | 111997.8 | 31.5 | 6.3492E-05 | 3.233617 | 20098.08 | 0.007056 | 0.011673 | 6305.328 |
| 38 | 57.1 | 3 | 92 | 109536.3 | 32.1 | 6.2305E-05 | 3.173175 | 19722.41 | 0.007327 | 0.011609 | 6187.471 |
| 38.6 | 56.7 | 5.5 | 89.5 | 103382.6 | 34.14 | 5.8582E-05 | 2.983565 | 18543.92 | 0.007854 | 0.012345 | 5817.745 |
| 39.5 | 55.6 | 8.5 | 86.5 | 95998.11 | 34.5 | 5.7971E-05 | 2.952433 | 18350.42 | 0.007134 | 0.012186 | 5757.039 |
| 39.6 | 54.6 | 9 | 86.2 | 95013.51 | 34.6 | 5.7803E-05 | 2.9439 | 18297.38 | 0.006686 | 0.012768 | 5740.4 |
| 40 | 55.2 | 12.5 | 82.5 | 86152.15 | 36.5 | 5.4795E-05 | 2.790655 | 17344.92 | 0.007539 | 0.01167 | 5441.584 |
| 40.2 | 55.2 | 10.7 | 84.8 | 91198.2 | 37.05 | 5.3981E-05 | 2.749229 | 17087.43 | 0.007666 | 0.013582 | 5360.805 |
| 40.3 | 55.3 | 12 | 83 | 87382.89 | 37.3 | 5.3619E-05 | 2.730802 | 16972.91 | 0.00777 | 0.012692 | 5324.875 |
| 41 | 54.2 | 14.5 | 80.5 | 81229.17 | 38.2 | 5.2356E-05 | 2.666464 | 16573.02 | 0.007171 | 0.012993 | 5199.42 |
| 41 | 54.2 | 14 | 81 | 82459.91 | 40 | 0.00005 | 2.546473 | 15827.24 | 0.007863 | 0.014644 | 4965.446 |
| 41.8 | 53.8 | 18 | 77 | 72613.95 | 43.2 | 4.6296E-05 | 2.357845 | 14654.85 | 0.008338 | 0.014642 | 4597.635 |
| 42 | 53.4 | 19.5 | 75.5 | 68921.72 | 43.4 | 4.6083E-05 | 2.34698 | 14587.31 | 0.007994 | 0.014015 | 4576.448 |
| 43.2 | 52.5 | 24.9 | 71 | 56737.34 | 47.35 | 4.2239E-05 | 2.151192 | 13370.42 | 0.007763 | 0.013841 | 4194.674 |
| 43.7 | 52 | 27 | 69 | 51691.29 | 51.3 | 3.8986E-05 | 1.985554 | 12340.93 | 0.008132 | 0.015061 | 3871.693 |
| 43.8 | 51.9 | 28 | 68 | 49229.8 | 55.2 | 3.6232E-05 | 1.84527 | 11469.01 | 0.009189 | 0.016269 | 3598.149 |
| 44.8 | 51 | 33 | 63 | 36922.35 | 58.5 | 3.4188E-05 | 1.741178 | 10822.04 | 0.007899 | 0.013461 | 3395.177 |
| 45.4 | 50.5 | 34.5 | 61.5 | 33230.11 | 67.75 | 2.952E-05 | 1.503453 | 9344.494 | 0.008715 | 0.017503 | 2931.628 |
| 46.3 | 49.7 | 39.5 | 56.5 | 20922.66 | 85 | 2.3529E-05 | 1.19834 | 7448.111 | 0.009146 | 0.01657 | 2336.68 |
| 46 | 50 | 39.5 | 56.7 | 21168.81 | 87 | 2.2989E-05 | 1.170792 | 7276.89 | 0.011272 | 0.015149 | 2282.964 |
| 47.9 | 48.3 | 46.9 | 49.1 | 2707.639 | 300 | 6.6667E-06 | 0.33953 | 2110.298 | 0.013403 | 0.028762 | 662.0594 |

**Table A.3 Experimental data for Spacer Length=4R, Curvature Radius=25.4mm, Number of bend=15**

| Straight pressure reading | | Full pressure reading. | | Total pressure | Time (Sec.) | Flow rate | Velocity | Reynolds no., Re | $f_S$ | $f_B$ | Dean no. |
|---|---|---|---|---|---|---|---|---|---|---|---|
| Right(cm) | left(cm) | right(cm) | left(cm) | $N/m^2$(Pa) | | $(m^3/sec)$ | m/sec | | | | |
| 40.2 | 59.2 | 0 | 99.6 | 122582.1962 | 31.2 | 6.41026E-05 | 3.264709 | 20291.33 | 0.006886 | 0.01359 | 6365.956 |
| 40 | 59.6 | 1.5 | 98 | 118766.8869 | 34 | 5.88235E-05 | 2.995851 | 18620.28 | 0.008435 | 0.014852 | 5841.701 |
| 42.3 | 57.3 | 9.4 | 89.8 | 98951.89334 | 34.5 | 5.7971E-05 | 2.952433 | 18350.42 | 0.006647 | 0.013642 | 5757.039 |
| 38 | 57.1 | 7 | 88 | 99690.3403 | 35.3 | 5.66572E-05 | 2.885522 | 17934.55 | 0.008861 | 0.011558 | 5626.567 |
| 41.9 | 57.9 | 9.6 | 90 | 98951.89334 | 35.6 | 5.61798E-05 | 2.861206 | 17783.41 | 0.007549 | 0.013804 | 5579.153 |
| 42.3 | 57.5 | 10 | 89 | 97228.85042 | 35.75 | 5.59441E-05 | 2.849201 | 17708.8 | 0.007232 | 0.014058 | 5555.743 |
| 41.1 | 58.7 | 13 | 87 | 91075.12571 | 37.1 | 5.39084E-05 | 2.745524 | 17064.41 | 0.009019 | 0.011546 | 5353.58 |
| 42 | 58 | 15 | 85 | 86152.14594 | 38.8 | 5.15464E-05 | 2.62523 | 16316.74 | 0.008968 | 0.012502 | 5119.016 |
| 43.5 | 56.5 | 16 | 84 | 83690.65606 | 39.5 | 5.06329E-05 | 2.578707 | 16027.58 | 0.007551 | 0.014846 | 5028.299 |
| 43.2 | 56.8 | 20 | 80 | 73844.69652 | 42 | 4.7619E-05 | 2.425213 | 15073.56 | 0.008932 | 0.012671 | 4728.996 |
| 44.4 | 55.4 | 19.8 | 80.2 | 74336.9945 | 42.1 | 4.75059E-05 | 2.419452 | 15037.75 | 0.007259 | 0.015532 | 4717.763 |
| 44 | 56 | 20.8 | 79 | 71629.35562 | 43.4 | 4.60829E-05 | 2.34698 | 14587.31 | 0.008415 | 0.014403 | 4576.448 |
| 45.2 | 55 | 24 | 76 | 63998.73698 | 45.6 | 4.38596E-05 | 2.233748 | 13883.54 | 0.007587 | 0.015298 | 4355.654 |
| 45.3 | 54.7 | 25.4 | 74.8 | 60798.80013 | 48.2 | 4.14938E-05 | 2.113256 | 13134.64 | 0.00813 | 0.016118 | 4120.702 |
| 43.8 | 54.4 | 27.4 | 73 | 56121.96936 | 50 | 0.00004 | 2.037179 | 12661.79 | 0.009866 | 0.013272 | 3972.357 |
| 46 | 54.2 | 28 | 72 | 54152.77745 | 52.2 | 3.83142E-05 | 1.95132 | 12128.15 | 0.008319 | 0.017105 | 3804.939 |
| 46.6 | 53.6 | 31.5 | 68.5 | 45537.56285 | 55.75 | 3.58744E-05 | 1.827066 | 11355.86 | 0.0081 | 0.016222 | 3562.652 |
| 46.7 | 53.5 | 32 | 68.4 | 44799.11589 | 56 | 3.57143E-05 | 1.818909 | 11305.17 | 0.007939 | 0.016257 | 3546.747 |
| 47 | 53.2 | 34 | 66.2 | 39629.98713 | 60.5 | 3.30579E-05 | 1.683619 | 10464.29 | 0.008449 | 0.0164 | 3282.939 |
| 47.1 | 53.3 | 34.2 | 66.4 | 39629.98713 | 62 | 3.22581E-05 | 1.642886 | 10211.12 | 0.008873 | 0.017224 | 3203.513 |
| 49.5 | 51.1 | 46.1 | 54.5 | 10338.25751 | 131.4 | 1.52207E-05 | 0.775182 | 4818.032 | 0.010285 | 0.020353 | 1511.551 |
| 49.8 | 50.8 | 47.6 | 53 | 6646.022687 | 170.6 | 1.17233E-05 | 0.597063 | 3710.958 | 0.010836 | 0.022528 | 1164.231 |
| 49.9 | 50.7 | 48.1 | 52.5 | 5415.277745 | 190 | 1.05263E-05 | 0.5361 | 3332.05 | 0.010752 | 0.023073 | 1045.357 |

**Table A.4 Experimental data for Spacer Length=4R, Curvature Radius=25.4mm, Number of bend=13**

| Straight pressure | | Full pressure red. | | Total pressure | Time | Flow rate | Velocity | Reynolds | | | Dean |
|---|---|---|---|---|---|---|---|---|---|---|---|
| Right(cm) | left(cm) | right(cm) | left(cm) | $N/m^2(Pa)$ | (*Sec.*) | ($m^3/sec$) | (*m/sec*) | no., *Re* | $f_S$ | $f_B$ | no. |
| 39.6 | 60 | -0.5 | 100 | 123689.8667 | 31 | 6.45161E-05 | 3.285772 | 20422.24 | 0.007299 | 0.013724 | 6407.027 |
| 40.4 | 59.2 | -0.4 | 100 | 123566.7922 | 32.3 | 6.19195E-05 | 3.153527 | 19600.29 | 0.007302 | 0.016062 | 6149.159 |
| 39 | 60.8 | 2.5 | 96.5 | 115690.0245 | 32.75 | 6.10687E-05 | 3.110196 | 19330.98 | 0.008705 | 0.012243 | 6064.667 |
| 41.5 | 58.3 | 6 | 94 | 108305.5549 | 34.9 | 5.73066E-05 | 2.918594 | 18140.1 | 0.007618 | 0.016156 | 5691.055 |
| 41.6 | 57.8 | 7.5 | 91.5 | 103382.5751 | 35 | 5.71429E-05 | 2.910255 | 18088.27 | 0.007388 | 0.015367 | 5674.795 |
| 43.2 | 56.6 | 15.5 | 84.5 | 84921.401 | 39 | 5.12821E-05 | 2.611767 | 16233.06 | 0.007588 | 0.015572 | 5092.765 |
| 43.5 | 56.5 | 17.5 | 82.5 | 79998.42123 | 39.5 | 5.06329E-05 | 2.578707 | 16027.58 | 0.007551 | 0.014628 | 5028.299 |
| 43.9 | 56.1 | 18.5 | 81.5 | 77536.93135 | 41 | 4.87805E-05 | 2.484364 | 15441.21 | 0.007635 | 0.015755 | 4844.337 |
| 41.4 | 58.6 | 18.8 | 80.8 | 76306.1864 | 41.2 | 4.85437E-05 | 2.472304 | 15366.25 | 0.01087 | 0.009358 | 4820.821 |
| 43.6 | 56.6 | 21 | 79 | 71383.20664 | 43.6 | 4.58716E-05 | 2.336214 | 14520.4 | 0.0092 | 0.014001 | 4555.455 |
| 45 | 55 | 25 | 75 | 61537.2471 | 45.2 | 4.42478E-05 | 2.253516 | 14006.4 | 0.007606 | 0.014734 | 4394.2 |
| 46.5 | 53.7 | 32.8 | 67.8 | 43076.07297 | 54.5 | 3.66972E-05 | 1.868971 | 11616.32 | 0.007962 | 0.01457 | 3644.364 |
| 46.3 | 54 | 32 | 68.2 | 44552.9669 | 55 | 3.63636E-05 | 1.85198 | 11510.72 | 0.008672 | 0.0148 | 3611.233 |
| 46.5 | 53.5 | 31.5 | 68.5 | 45537.56285 | 56 | 3.57143E-05 | 1.818909 | 11305.17 | 0.008173 | 0.017632 | 3546.747 |
| 45.4 | 54.8 | 33.2 | 67 | 41599.17904 | 58.6 | 3.41297E-05 | 1.738207 | 10803.57 | 0.012018 | 0.010264 | 3389.383 |
| 47.7 | 52.7 | 37.1 | 63.3 | 32245.51748 | 68.2 | 2.93255E-05 | 1.493533 | 9282.837 | 0.008658 | 0.018374 | 2912.285 |
| 47.7 | 52.8 | 38 | 62.6 | 30276.32557 | 70 | 2.85714E-05 | 1.455128 | 9044.135 | 0.009304 | 0.016756 | 2837.398 |
| 48.2 | 52.2 | 39.8 | 60.6 | 25599.49479 | 78.1 | 2.56082E-05 | 1.304212 | 8106.139 | 0.009084 | 0.018996 | 2543.122 |
| 48.6 | 52 | 43.5 | 57.3 | 16984.2802 | 96 | 2.08333E-05 | 1.06103 | 6594.682 | 0.011666 | 0.01413 | 2068.936 |
| 49.1 | 52 | 45.3 | 55.3 | 12307.44942 | 118 | 1.69492E-05 | 0.863211 | 5365.165 | 0.015033 | 0.01113 | 1683.202 |
| 49.3 | 51.3 | 45.8 | 54.8 | 11076.70448 | 133.1 | 1.50263E-05 | 0.765281 | 4756.495 | 0.013191 | 0.020465 | 1492.245 |
| 49.5 | 51 | 46.8 | 53.8 | 8615.214594 | 140 | 1.42857E-05 | 0.727564 | 4522.068 | 0.010946 | 0.018389 | 1418.699 |
| 49.8 | 50.8 | 47.5 | 53 | 6769.097181 | 173.4 | 1.1534E-05 | 0.587422 | 3651.035 | 0.011194 | 0.026 | 1145.432 |
| 50.2 | 50.4 | 49.5 | 51.1 | 1969.191907 | 347.5 | 5.7554E-06 | 0.293119 | 1821.84 | 0.008991 | 0.03822 | 571.5621 |

## Table A.5 Experimental data for Spacer Length=4R, Curvature Radius=25.4mm, Number of bend=11

| Straight pressure reading | | Full pressure reading. | | Total pressure | Time | Flow rate | Velocity | Reynolds | | | Dean |
|---|---|---|---|---|---|---|---|---|---|---|---|
| Right(cm) | left(cm) | right(cm) | left(cm) | $N/m^2(Pa)$ | (*Sec.*) | ($m^3/sec$) | (*m/sec*) | no. *Re* | $f_S$ | $f_B$ | no. |
| 36.4 | 58.6 | -3.5 | 100.5 | 127997.474 | 29.4 | 6.8027E-05 | 3.464589 | 21533.66 | 0.007144 | 0.011438 | 6755.708 |
| 40.8 | 58.8 | 3.4 | 96 | 113966.9816 | 32.2 | 6.2112E-05 | 3.163321 | 19661.16 | 0.006948 | 0.01326 | 6168.256 |
| 38.6 | 56.8 | 4.5 | 91.1 | 106582.512 | 33.5 | 5.9701E-05 | 3.040565 | 18898.19 | 0.007604 | 0.012549 | 5928.89 |
| 40.8 | 58.8 | 5.4 | 84 | 96736.55244 | 34 | 5.8824E-05 | 2.995851 | 18620.28 | 0.007747 | 0.010757 | 5841.701 |
| 40.2 | 55.4 | 9.8 | 85.8 | 93536.61559 | 36.3 | 5.5096E-05 | 2.806031 | 17440.48 | 0.007457 | 0.01351 | 5471.566 |
| 42.5 | 57.3 | 11.5 | 88.3 | 94521.21155 | 37 | 5.4054E-05 | 2.752944 | 17110.53 | 0.007543 | 0.014621 | 5368.049 |
| 42.6 | 57.4 | 13 | 87 | 91075.12571 | 39.36 | 5.0813E-05 | 2.587879 | 16084.59 | 0.008536 | 0.015466 | 5046.185 |
| 44.9 | 54.7 | 13.8 | 81.8 | 83690.65606 | 39.4 | 5.0761E-05 | 2.585252 | 16068.26 | 0.005664 | 0.0176 | 5041.062 |
| 43.6 | 56.4 | 17 | 83 | 81229.16617 | 40.6 | 4.9261E-05 | 2.508841 | 15593.34 | 0.007855 | 0.015052 | 4892.065 |
| 43.8 | 56 | 19 | 81 | 76306.1864 | 42 | 4.7619E-05 | 2.425213 | 15073.56 | 0.008012 | 0.014955 | 4728.996 |
| 44.5 | 55.7 | 21 | 79 | 71383.20664 | 43.27 | 4.6221E-05 | 2.354031 | 14631.14 | 0.007807 | 0.015076 | 4590.197 |
| 44.3 | 55.7 | 20 | 80 | 73844.69652 | 43.6 | 4.5872E-05 | 2.336214 | 14520.4 | 0.008068 | 0.016037 | 4555.455 |
| 43.4 | 52.4 | 24.5 | 71.5 | 57845.01227 | 49.5 | 4.0404E-05 | 2.057756 | 12789.69 | 0.00821 | 0.016094 | 4012.481 |
| 43.4 | 52.6 | 25 | 71 | 56614.26733 | 50 | 0.00004 | 2.037179 | 12661.79 | 0.008563 | 0.015514 | 3972.357 |
| 45.7 | 54.5 | 28.5 | 71.7 | 53168.18149 | 52.5 | 3.8095E-05 | 1.94017 | 12058.85 | 0.00903 | 0.015812 | 3783.197 |
| 46.5 | 53.9 | 31.4 | 69 | 46276.00982 | 55 | 3.6364E-05 | 1.85198 | 11510.72 | 0.008334 | 0.015551 | 3611.233 |
| 44.7 | 51.5 | 31.5 | 64.9 | 41106.88106 | 58.9 | 3.3956E-05 | 1.729354 | 10748.55 | 0.008783 | 0.015395 | 3372.119 |
| 44.1 | 51.9 | 28.6 | 67.4 | 47752.90375 | 60 | 3.3333E-05 | 1.697649 | 10551.49 | 0.010454 | 0.018762 | 3310.297 |
| 46.5 | 53.7 | 33.4 | 57 | 29045.58063 | 60 | 3.3333E-05 | 1.697649 | 10551.49 | 0.00965 | 0.006377 | 3310.297 |
| 45.4 | 50.8 | 35.2 | 61 | 31753.2195 | 69.8 | 2.8653E-05 | 1.459297 | 9070.05 | 0.009795 | 0.016292 | 2845.528 |
| 45.9 | 50.3 | 37.4 | 59 | 26584.09075 | 76.3 | 2.6212E-05 | 1.334979 | 8297.372 | 0.009537 | 0.016699 | 2603.117 |
| 46.1 | 50.2 | 38.9 | 57.5 | 22891.85592 | 85.3 | 2.3447E-05 | 1.194126 | 7421.916 | 0.011106 | 0.016683 | 2328.462 |
| 48.5 | 51.9 | 41.8 | 58.8 | 20922.66401 | 89.3 | 2.2396E-05 | 1.140637 | 7089.468 | 0.010094 | 0.018289 | 2224.164 |
| 49.2 | 51.2 | 45.3 | 55.5 | 12553.59841 | 117.6 | 1.7007E-05 | 0.866147 | 5383.414 | 0.010298 | 0.019345 | 1688.927 |
| 49.9 | 50.9 | 47.8 | 53 | 6399.873698 | 179 | 1.1173E-05 | 0.569044 | 3536.813 | 0.011929 | 0.023207 | 1109.597 |
| 49.8 | 50.8 | 48 | 52.8 | 5907.575722 | 186.8 | 1.0707E-05 | 0.545283 | 3389.13 | 0.012991 | 0.021801 | 1063.265 |

## Table A.6 Experimental data for Spacer Length=4R, Curvature Radius=25.4mm, Number of bend=9

| Straight pressure reading | | Full pressure red. | | Total pressure | Time | Flow rate | Velocity | Reynolds no., *Re* | $f_S$ | $f_B$ | Dean no. |
|---|---|---|---|---|---|---|---|---|---|---|---|
| Right(cm) | left(cm) | right(cm) | left(cm) | $N/m^2(Pa)$ | *(Sec.)* | *(m3/sec)* | *(m/sec)* | | | | |
| 37 | 58 | -3.5 | 99.5 | 126766.729 | 30 | 6.66667E-05 | 3.395298 | 21102.98 | 0.007036 | 0.015821 | 6620.594 |
| 37.2 | 57.8 | -0.5 | 95.5 | 118151.5144 | 31.9 | 6.26959E-05 | 3.19307 | 19846.06 | 0.007804 | 0.015421 | 6226.264 |
| 38.8 | 56.2 | 4 | 91 | 107074.81 | 34.3 | 5.8309E-05 | 2.969648 | 18457.42 | 0.007621 | 0.017944 | 5790.607 |
| 39 | 56 | 6 | 89 | 102151.8302 | 35 | 5.71429E-05 | 2.910255 | 18088.27 | 0.007753 | 0.017239 | 5674.795 |
| 39.7 | 55.3 | 12.5 | 82.5 | 86152.14594 | 38 | 5.26316E-05 | 2.680498 | 16660.25 | 0.008387 | 0.014955 | 5226.785 |
| 41.2 | 54.8 | 13 | 82 | 84921.401 | 38.2 | 5.2356E-05 | 2.666464 | 16573.02 | 0.007389 | 0.018001 | 5199.42 |
| 41.3 | 54.5 | 15 | 80 | 79998.42123 | 40 | 0.00005 | 2.546473 | 15827.24 | 0.007863 | 0.01785 | 4965.446 |
| 41.3 | 54.3 | 18.5 | 77 | 71998.57911 | 42.5 | 4.70588E-05 | 2.396681 | 14896.22 | 0.008742 | 0.015714 | 4673.361 |
| 42.5 | 53.1 | 23.5 | 72 | 59691.12969 | 49.3 | 4.0568E-05 | 2.066104 | 12841.57 | 0.009592 | 0.018048 | 4028.759 |
| 43.5 | 52.4 | 26 | 70 | 54152.77745 | 50 | 0.00004 | 2.037179 | 12661.79 | 0.008284 | 0.018985 | 3972.357 |
| 43.7 | 52.3 | 27 | 69 | 51691.28756 | 51 | 3.92157E-05 | 1.997234 | 12413.52 | 0.008328 | 0.018529 | 3894.467 |
| 44 | 51 | 27.4 | 68.4 | 50460.54262 | 52 | 3.84615E-05 | 1.958825 | 12174.8 | 0.007047 | 0.02332 | 3819.574 |
| 44.1 | 51.9 | 28.5 | 67.5 | 47999.05274 | 53.87 | 3.71264E-05 | 1.890828 | 11752.17 | 0.008427 | 0.019842 | 3686.984 |
| 44.3 | 51.5 | 30 | 66 | 44306.81791 | 57.68 | 3.46741E-05 | 1.765931 | 10975.89 | 0.008918 | 0.020998 | 3443.444 |
| 44.8 | 51.2 | 32.5 | 63.5 | 38153.0932 | 61.9 | 3.23102E-05 | 1.64554 | 10227.62 | 0.00913 | 0.019907 | 3208.689 |
| 45.5 | 50.5 | 35.3 | 60.7 | 31260.92153 | 68.9 | 2.90276E-05 | 1.478359 | 9188.526 | 0.008837 | 0.021594 | 2882.697 |
| 45.9 | 50.1 | 37.5 | 58.6 | 25968.71828 | 77 | 2.5974E-05 | 1.322843 | 8221.941 | 0.009271 | 0.022074 | 2579.452 |
| 46 | 50 | 38 | 58 | 24614.89884 | 79 | 2.53165E-05 | 1.289353 | 8013.791 | 0.009294 | 0.021883 | 2514.15 |
| 46.5 | 49.5 | 40 | 56 | 19691.91907 | 93.8 | 2.1322E-05 | 1.085916 | 6749.355 | 0.009827 | 0.026786 | 2117.461 |
| 46.8 | 49.3 | 42.2 | 53.8 | 14276.64133 | 104 | 1.92308E-05 | 0.979413 | 6087.399 | 0.010067 | 0.019666 | 1909.787 |
| 46.7 | 49.3 | 42.5 | 53.5 | 13538.19436 | 110.5 | 1.80995E-05 | 0.9218 | 5729.316 | 0.011819 | 0.017701 | 1797.446 |
| 47 | 49 | 43.5 | 52.5 | 11076.70448 | 123.6 | 1.61812E-05 | 0.824101 | 5122.083 | 0.011375 | 0.020447 | 1606.94 |

## Table A.7 Experimental data for Spacer Length=3R, Curvature Radius=25.4mm, Number of bend=9

| Straight pressure | | Full pressure red. | | Total pressure | Time | Flow rate | Velocity | Reynolds no. *Re* | $f_S$ | $f_B$ | Dean no. |
|---|---|---|---|---|---|---|---|---|---|---|---|
| Right(cm) | left(cm) | right(cm) | left(cm) | $N/m^2(Pa)$ | *(Sec.)* | $(m^3/sec)$ | *(m/sec)* | | | | |
| 37.7 | 58.2 | -1.5 | 97.5 | 121843.7493 | 31.45 | 6.359E-05 | 3.23876 | 20130 | 0.00755 | 0.01282 | 6315.35 |
| 38.8 | 57.2 | 3 | 83 | 98459.59536 | 32.7 | 6.116E-05 | 3.11495 | 19360.5 | 0.00732 | 0.01008 | 6073.94 |
| 39 | 57 | 7 | 89 | 100921.0852 | 35.1 | 5.698E-05 | 2.90196 | 18036.7 | 0.00826 | 0.01251 | 5658.63 |
| 39.7 | 56.3 | 8 | 88.5 | 99074.96783 | 35.8 | 5.587E-05 | 2.84522 | 17684.1 | 0.00792 | 0.01355 | 5547.98 |
| 40.5 | 55.5 | 10.5 | 85.5 | 92305.87065 | 36.6 | 5.464E-05 | 2.78303 | 17297.5 | 0.00748 | 0.01355 | 5426.72 |
| 40.2 | 56 | 8.8 | 87 | 96244.25446 | 36.8 | 5.435E-05 | 2.76791 | 17203.5 | 0.00797 | 0.01416 | 5397.22 |
| 39.5 | 56.6 | 14.5 | 81.5 | 82459.91111 | 40.1 | 4.988E-05 | 2.54012 | 15787.8 | 0.01024 | 0.01115 | 4953.06 |
| 41.2 | 54.8 | 15.5 | 80.5 | 79998.42123 | 40.2 | 4.975E-05 | 2.5338 | 15748.5 | 0.00818 | 0.01362 | 4940.74 |
| 41 | 55 | 15 | 81 | 81229.16617 | 40.4 | 4.95E-05 | 2.52126 | 15670.5 | 0.00851 | 0.01379 | 4916.28 |
| 41.4 | 55.8 | 16.5 | 79.5 | 77536.93135 | 40.48 | 4.941E-05 | 2.51628 | 15639.6 | 0.00878 | 0.01225 | 4906.57 |
| 42 | 54.2 | 18 | 78 | 73844.69652 | 42.4 | 4.717E-05 | 2.40233 | 14931.4 | 0.00817 | 0.01435 | 4684.38 |
| 41.2 | 55 | 20.5 | 75.7 | 67937.1208 | 44.8 | 4.464E-05 | 2.27364 | 14131.5 | 0.01031 | 0.01179 | 4433.43 |
| 42.8 | 53.4 | 22.5 | 73.5 | 62767.99204 | 45.75 | 4.372E-05 | 2.22642 | 13838 | 0.00826 | 0.01392 | 4341.37 |
| 42.7 | 53.5 | 22 | 74 | 63998.73698 | 45.8 | 4.367E-05 | 2.22399 | 13822.9 | 0.00843 | 0.01424 | 4336.63 |
| 43.3 | 53 | 24.5 | 71.5 | 57845.01227 | 48.9 | 4.09E-05 | 2.083 | 12946.6 | 0.00864 | 0.01475 | 4061.71 |
| 44 | 52.2 | 29 | 67.2 | 47014.45678 | 52.85 | 3.784E-05 | 1.92732 | 11979 | 0.00853 | 0.0135 | 3758.14 |
| 44.2 | 52 | 29 | 67 | 46768.3078 | 54.13 | 3.695E-05 | 1.88175 | 11695.7 | 0.00851 | 0.01469 | 3669.27 |
| 44.3 | 52 | 29.5 | 66.7 | 45783.71184 | 54.15 | 3.693E-05 | 1.88105 | 11691.4 | 0.00841 | 0.01428 | 3667.92 |
| 45 | 51 | 33 | 63.3 | 37291.57174 | 63.3 | 3.16E-05 | 1.60915 | 10001.4 | 0.00895 | 0.01652 | 3137.72 |
| 45.4 | 51 | 34.5 | 61.8 | 33599.33692 | 67 | 2.985E-05 | 1.52028 | 9449.1 | 0.00936 | 0.01617 | 2964.45 |
| 46.2 | 50.2 | 37.5 | 59 | 26461.01625 | 77.4 | 2.584E-05 | 1.31601 | 8179.45 | 0.00892 | 0.0184 | 2566.12 |
| 47 | 49.5 | 42 | 54.5 | 15384.31178 | 103.7 | 1.929E-05 | 0.98225 | 6105.01 | 0.01001 | 0.01813 | 1915.31 |
| 47.5 | 49 | 44 | 52.5 | 10461.33201 | 126 | 1.587E-05 | 0.8084 | 5024.52 | 0.00887 | 0.02001 | 1576.33 |
| 48 | 48.5 | 46.5 | 50 | 4307.607297 | 216.8 | 9.225E-06 | 0.46983 | 2920.15 | 0.00875 | 0.02755 | 916.134 |

## Table A.8 Experimental data for Spacer Length=2R, Curvature Radius=25.4mm, Number of bend=9

| Straight pressure | | Full pressure red. | | Total pressure | Time | Flow rate | Velocity | Reynolds no. *Re* | $f_S$ | $f_B$ | Dean no. |
|---|---|---|---|---|---|---|---|---|---|---|---|
| Right(cm) | left(cm) | right(cm) | left(cm) | $N/m^2(Pa)$ | *(Sec.)* | *(m3/sec)* | *(m/sec)* | | | | |
| 37.6 | 58 | -2 | 98 | 123074.4942 | 32 | 0.0000625 | 3.183091 | 19784.05 | 0.007777 | 0.013581 | 6206.807 |
| 38.3 | 57.5 | 1 | 94.8 | 115443.8756 | 32.8 | 6.0976E-05 | 3.105455 | 19301.51 | 0.00769 | 0.013344 | 6055.422 |
| 39 | 56.9 | 3.5 | 92.4 | 109413.2253 | 34.29 | 5.8326E-05 | 2.970514 | 18462.8 | 0.007836 | 0.014021 | 5792.296 |
| 39.2 | 56.8 | 7 | 89 | 100921.0852 | 35 | 5.7143E-05 | 2.910255 | 18088.27 | 0.008027 | 0.012714 | 5674.795 |
| 40 | 55.9 | 9 | 86.8 | 95751.95649 | 36.15 | 5.5325E-05 | 2.817674 | 17512.85 | 0.007736 | 0.013463 | 5494.269 |
| 40.5 | 55.5 | 13 | 83 | 86152.14594 | 37.64 | 5.3135E-05 | 2.706135 | 16819.59 | 0.007912 | 0.012572 | 5276.775 |
| 41.1 | 54.8 | 12 | 83.6 | 88121.33785 | 39.35 | 5.0826E-05 | 2.588537 | 16088.68 | 0.007898 | 0.015503 | 5047.467 |
| 41 | 54.8 | 14 | 81.8 | 83444.50707 | 39.47 | 5.0671E-05 | 2.580667 | 16039.76 | 0.008004 | 0.014036 | 5032.121 |
| 40.8 | 55.4 | 15 | 81 | 81229.16617 | 39.8 | 5.0251E-05 | 2.559269 | 15906.77 | 0.00861 | 0.012841 | 4990.398 |
| 40.9 | 55.3 | 16 | 80 | 78767.67629 | 40 | 0.00005 | 2.546473 | 15827.24 | 0.008578 | 0.012356 | 4965.446 |
| 42.2 | 53.8 | 18.5 | 77.5 | 72613.95158 | 44.5 | 4.4944E-05 | 2.288965 | 14226.73 | 0.008552 | 0.015987 | 4463.322 |
| 42.3 | 53.6 | 20.8 | 75 | 66706.37586 | 45.2 | 4.4248E-05 | 2.253516 | 14006.4 | 0.008595 | 0.014403 | 4394.2 |
| 42.8 | 53.4 | 22.2 | 74 | 63752.588 | 46.47 | 4.3039E-05 | 2.191929 | 13623.62 | 0.008522 | 0.014795 | 4274.109 |
| 43 | 53 | 23.5 | 72.5 | 60306.50216 | 47.25 | 4.2328E-05 | 2.155744 | 13398.72 | 0.008312 | 0.014504 | 4203.552 |
| 43.8 | 52.4 | 28.8 | 67.4 | 47506.75476 | 51.4 | 3.8911E-05 | 1.981691 | 12316.92 | 0.008459 | 0.012434 | 3864.16 |
| 44 | 52 | 27 | 69 | 51691.28756 | 52.76 | 3.7908E-05 | 1.930609 | 11999.42 | 0.008291 | 0.016406 | 3764.553 |
| 44.7 | 51.5 | 30.5 | 65.7 | 43322.22196 | 59 | 3.3898E-05 | 1.726422 | 10730.33 | 0.008813 | 0.017006 | 3366.404 |
| 44.8 | 51.3 | 31.5 | 64.5 | 40614.58309 | 61 | 3.2787E-05 | 1.669818 | 10378.52 | 0.009005 | 0.016777 | 3256.03 |
| 45.5 | 51.7 | 34 | 62.2 | 34707.00736 | 66.2 | 3.0211E-05 | 1.538654 | 9563.285 | 0.010116 | 0.015275 | 3000.269 |
| 45.7 | 50.5 | 36 | 60.3 | 29907.10209 | 71.6 | 2.7933E-05 | 1.422611 | 8842.032 | 0.009161 | 0.016981 | 2773.992 |
| 46 | 50.3 | 37.5 | 58.8 | 26214.86726 | 86 | 2.3256E-05 | 1.184406 | 7361.505 | 0.01184 | 0.021084 | 2309.51 |
| 46.4 | 50 | 39.1 | 57.3 | 22399.55794 | 87 | 2.2989E-05 | 1.170792 | 7276.89 | 0.010145 | 0.018757 | 2282.964 |
| 47 | 49.4 | 41.7 | 54.7 | 15999.68425 | 102 | 1.9608E-05 | 0.998617 | 6206.759 | 0.009296 | 0.019431 | 1947.234 |
| 47.3 | 49.1 | 43.5 | 54.3 | 13292.04537 | 116 | 1.7241E-05 | 0.878094 | 5457.668 | 0.009017 | 0.022364 | 1712.223 |
| 47.8 | 48.8 | 46 | 50.4 | 5415.277745 | 186.6 | 1.0718E-05 | 0.545868 | 3392.762 | 0.012963 | 0.018289 | 1064.404 |
| 48.1 | 48.5 | 47.1 | 49.5 | 2953.787861 | 282.3 | 7.0847E-06 | 0.360818 | 2242.612 | 0.011868 | 0.029434 | 703.5701 |

## Table A.9 Experimental data for Spacer Length=R, Curvature Radius=25.4mm, Number of bend=9

| Straight pressure | | Full pressure red. | | Total pressure | Time | Flow rate | Velocity | Reynolds | | | Dean |
|---|---|---|---|---|---|---|---|---|---|---|---|
| Right(cm) | left(cm) | right(cm) | left(cm) | $N/m^2(Pa)$ | *(Sec.)* | $(m^3/sec)$ | *(m/sec)* | no. *Re* | $f_S$ | $f_B$ | no. |
| 43.2 | 63.3 | 5 | 101.5 | 118766.8869 | 32.85 | 6.0883E-05 | 3.100728 | 19272.13 | 0.008075 | 0.013557 | 6046.205 |
| 44 | 62.5 | 7 | 99.5 | 113843.9071 | 33.8 | 5.9172E-05 | 3.013578 | 18730.46 | 0.007869 | 0.014256 | 5876.267 |
| 44.7 | 62 | 10 | 96.7 | 106705.5865 | 35.4 | 5.6497E-05 | 2.877371 | 17883.88 | 0.008071 | 0.014686 | 5610.673 |
| 45 | 61.5 | 10.5 | 96 | 105228.6925 | 35.8 | 5.5866E-05 | 2.845221 | 17684.06 | 0.007873 | 0.015221 | 5547.984 |
| 44.8 | 61.7 | 13 | 93.5 | 99074.96783 | 36.2 | 5.5249E-05 | 2.813782 | 17488.66 | 0.008245 | 0.013634 | 5486.68 |
| 45.6 | 61 | 15 | 91.6 | 94275.06256 | 37.82 | 5.2882E-05 | 2.693256 | 16739.54 | 0.008201 | 0.014716 | 5251.661 |
| 46 | 60.8 | 19.5 | 87.2 | 83321.43257 | 38.83 | 5.1507E-05 | 2.623202 | 16304.13 | 0.008308 | 0.012689 | 5115.061 |
| 46.5 | 60.1 | 21.6 | 85 | 78029.22932 | 40.96 | 4.8828E-05 | 2.48679 | 15456.29 | 0.008495 | 0.013471 | 4849.068 |
| 47.7 | 59.3 | 23 | 84 | 75075.44146 | 42.8 | 4.6729E-05 | 2.379881 | 14791.81 | 0.007911 | 0.015701 | 4640.603 |
| 48.5 | 58.5 | 27.5 | 79.5 | 63998.73698 | 47.2 | 4.2373E-05 | 2.158028 | 13412.91 | 0.008294 | 0.016136 | 4208.005 |
| 48 | 59.2 | 33 | 74.4 | 50952.8406 | 52.3 | 3.8241E-05 | 1.947589 | 12104.96 | 0.011405 | 0.010728 | 3797.664 |
| 49.5 | 57.5 | 32.5 | 74.5 | 51691.28756 | 53.5 | 3.7383E-05 | 1.903905 | 11833.45 | 0.008525 | 0.01687 | 3712.483 |
| 49.9 | 57.3 | 34.6 | 72.4 | 46522.15881 | 56.7 | 3.5273E-05 | 1.796454 | 11165.6 | 0.008857 | 0.016687 | 3502.96 |
| 49 | 58.5 | 35.7 | 71.5 | 44060.66892 | 58.3 | 3.4305E-05 | 1.747151 | 10859.17 | 0.012021 | 0.011886 | 3406.824 |
| 50.1 | 57 | 37 | 70 | 40614.58309 | 59.5 | 3.3613E-05 | 1.711915 | 10640.16 | 0.009094 | 0.015156 | 3338.115 |
| 50.5 | 56.6 | 38 | 69.1 | 38276.1677 | 63 | 3.1746E-05 | 1.616808 | 10049.04 | 0.009014 | 0.016924 | 3152.664 |
| 50.6 | 56.5 | 39 | 68 | 35691.60332 | 65.2 | 3.0675E-05 | 1.562253 | 9709.961 | 0.009338 | 0.016389 | 3046.286 |
| 51 | 56.5 | 40 | 67.5 | 33845.48591 | 70 | 2.8571E-05 | 1.455128 | 9044.135 | 0.010033 | 0.018179 | 2837.398 |
| 51.1 | 56.5 | 42.5 | 65 | 27691.7612 | 75.5 | 2.649E-05 | 1.349125 | 8385.291 | 0.01146 | 0.014381 | 2630.7 |
| 51.8 | 55.7 | 44.5 | 62.9 | 22645.70693 | 84.6 | 2.3641E-05 | 1.204006 | 7483.327 | 0.010392 | 0.016869 | 2347.728 |
| 51.7 | 55.8 | 46 | 61.5 | 19076.5466 | 91.86 | 2.1772E-05 | 1.10885 | 6891.895 | 0.01288 | 0.012839 | 2162.18 |
| 52.2 | 55.3 | 46.3 | 61 | 18091.95065 | 97 | 2.0619E-05 | 1.050092 | 6526.695 | 0.010859 | 0.017802 | 2047.606 |
| 52.5 | 55 | 48.2 | 59.3 | 13661.26886 | 114.27 | 1.7502E-05 | 0.891388 | 5540.295 | 0.012153 | 0.017471 | 1738.145 |
| 52.7 | 54.8 | 49.3 | 58.2 | 10953.62998 | 129 | 1.5504E-05 | 0.789604 | 4907.67 | 0.01301 | 0.016947 | 1539.673 |
| 52.8 | 54.7 | 49.7 | 57.8 | 9969.03403 | 137.5 | 1.4545E-05 | 0.740792 | 4604.287 | 0.013374 | 0.017645 | 1444.493 |
| 53.3 | 54.2 | 51.5 | 56 | 5538.352239 | 200 | 0.00001 | 0.509295 | 3165.447 | 0.013403 | 0.024283 | 993.0891 |

**Sample Calculation**

For $d$ = 5mm and 15 bends

Total pressure, $\Delta P_T = \rho g h_T$

$= 1000 \times 9.81\{98 - (-3.5)\}\left(\frac{13.6}{1} - 1\right) \times 10\text{^}-2$

$= 124920.61\ N/m^2$

$h_T = H_{13}\left(\frac{S_g}{S_w} - 1\right)$

$$Flowrate, Q = \frac{Volume}{Time(sce.)}$$

$$= \frac{1 \times 10^{-2}}{27.09}$$

$$= 7.3828 \times 10^{-5}\ m^3 / sce$$

Velocity,

$$v = \frac{Q}{A}$$

$$= \frac{7.3828 \times 10^{-5}}{1.963 \times 10^{-5}}$$

$$= 3.760019 m / s$$

Reynolds number,

$$Re = \frac{\rho v d}{\mu}$$

$$= \frac{1000 \times 3.760019 \times 5 \times 10^{-3}}{1.0028 \times 10^{-2}}$$

$$= 23269.85$$

Dean number is defined as, $D_n = Re\sqrt{\frac{d}{2R}}$

Theoretical straight friction factor,

$$f_s = \frac{0.0791}{(Re)^{0.25}}$$
$$= .0791 \times 23296.85^{-..25}$$
$$= 6.3982 \times 10^{-3}$$

Experimental straight friction factor, $f_s = \frac{2h_{12}gd}{4L_{12}v^2}$

$$= \frac{2 \times (59.68 - 35.3) \times 10^{-2} \times gd}{4L_{12}v^2}$$

$$= \frac{2 \times (59.68 - 35.3) \times 10^{-2} \times 9.81 \times .005}{4 \times 0.50 \times 3.760019^2}$$
$$= 6.6392 \times 10^{-3}$$

Bending friction factor,

$$f_B = \frac{\Delta P_{13} - \frac{4L_{st}\rho v^2 f_s}{2d}}{\frac{4L_c \rho v^2}{2d}}$$
$$= \frac{124920.61 - \frac{4 \times (290 \times .005 + 14 \times .0508) \times 1000 \times 3.760019^2 \times 6.6392 \times 10^{-3}}{2 \times .005}}{4 \times \frac{(15 \times \pi \times .0254 \times 3.760019^2)}{2 \times .005}}$$
$$= 8.377 \times 10^{-3}$$

# APPENDIX-B

## Uncertainty Analysis:

In the present experiment, each point was taken only once, and hence they were single sample experiment. A precise method of single sample uncertainty analysis has been described in the engineering literature by the works of Kline and McClintock [1953, 1988].

If a variable x, has a known uncertainty $W_1$, then the form of representing this variable and its uncertainty is,

$$x_1 = x_1 \text{ (measured)} \pm W_1 \qquad \text{(B-1)}$$

This statement should be interpreted to mean the following:

- The best estimate of $x_1$ is $x_1$ (measured).
- There is an uncertainty in $x_1$ that may be as varid as $\pm W_1$.
- The odds are 1 to 20 against the uncertainty of $x_1$ being larger than $\pm W_1$.

It is important to note that such specification can only be made by the experimenter based on the total laboratory experience.

Now, suppose, a set of measurement is made and the uncertainty in each measurement may be expressed with the same odds. These measurement are then used to calculate some desired result P using the independent variables $x_1, x_2, x_3 \ldots\ldots\ldots\ldots x_n$, where,

$$P = P(x_1, x_2, x_3 \ldots\ldots\ldots\ldots x_n) \qquad \text{(B-2)}$$

Let, $W_1, W_2, W_3 \ldots\ldots\ldots\ldots W_p$ be the uncertainties in the independent variables given with the same odds. Then the uncertainty $W_p$ in the result having these odds is given in Kline and McClintock as

$$W_P = \left[ \left( \frac{\partial P}{\partial x_1} W_1 \right)^2 + \left( \frac{\partial P}{\partial x_2} W_2 \right)^2 + \ldots\ldots\ldots\ldots + \left( \frac{\partial p}{\partial x_n} W_n \right)^2 \right]^{\frac{1}{2}} \qquad \text{(B-3)}$$

where the partial derivative of P with respect to $x_1$ is the sensitivity coefficient for the result P with to the measurement $x_1$. In most situation the overall uncertainty in a given result is dominated by only a few of its terms. Terms in the uncertainty equation that are smaller than the largest term by a factor of 3 or more can be usually be ignored (Moffat,1988). This is a natural consequence of the Root Sum Square (RSS) combination. Small terms have very small effects.

Sometimes the estimate is wanted as a fraction of reading rather than in engineering units. While this can always be calculated using equation B-3, it is also possible to do the calculation of relative uncertainty directly. In particular, whenever the equation describing the result is a pure product form such as equation B-4, then the relative uncertainty can be found directly. That is, if

$$P=P(x_1^a, x_2^b, x_3^c \ldots\ldots\ldots\ldots\ldots x_n^m) \tag{B-4}$$

Then,

$$\frac{W_P}{P}=\left[\left(a\frac{W_1}{x_1}\right)^2+\left(b\frac{W_2}{x_2}\right)^2+\ldots\ldots\ldots\ldots\ldots\ldots\ldots+\left(m\frac{W_n}{x_m}\right)^2\right]^{\frac{1}{2}} \tag{B-5}$$

**Uncertainty Analysis of Present Experimental Data**

For tube diameter, $d$ = 5mm and number of bend, $n$ =15 of test section

Uncertainty in manometer reading, $w_h = \pm 0.5$ mm

Uncertainty in measured volume, $w_v = \pm 5$ ml

Uncertainty in measured time, $w_t = \pm 0.1$ sec

Uncertainty in measured diameter, $w_D = \pm 0.1$ mm

Uncertainty in measured length, $w_{Lst} = \pm 1$mm

Temperature, T= 25 ±2.5ºC

Density of water, $\rho = a + bT + cT^2 + dT^3$ Here T is in K

$= 266.5 + 6.446(25 + 273) - .01788(25 + 273)^2 + 0.0000148(25 + 273)^3$

$= 266.5 + 6.446(298) - 0.01788 \times (298)^2 + 0.0000148 \times (298)^3$

$= 991.25 \text{ kg/m}^3$

$$\frac{\partial \rho}{\partial T} = b + 2cT + 3dT^2$$

$= 6.446 - 2 \times 0.01788 \times 298 + 3 \times 0.0000148 \times (298)^2$

$= - 0.2675$

Uncertainty in calculated density,

$$w_\rho = \frac{\partial \rho}{\partial T} w_T$$

$= - 0.2675 \times 2.5$

$= - 0.66875 \text{kg/m}^3$

Density of water, $\rho = 991.25 \pm 0.66875 \text{kg/m}^3$

Total pressure, $\Delta P_T = \rho g h_{13}$

Uncertainty in calculated pressure,

$$w_{\Delta P_T} = \left[ \left( \frac{\partial \Delta P}{\partial h} w_h \right)^2 + \left( \frac{\partial \Delta P}{\partial \rho} w_\rho \right)^2 \right]^{\frac{1}{2}}$$

$$= \left[ (\rho g w_h)^2 + (h g w_\rho)^2 \right]^{\frac{1}{2}}$$

$$= [(991.25 \times 9.81 \times 0.5 \times 10^{-3})^2 + (101.5 \times 10^{-2} \times 9.81 \times 0.66875)^2]^{\frac{1}{2}}$$

$$= 8.25 N/m^2$$

Total pressure, $\Delta P_T = 124920.61 \pm 8.25\ N/m^2$

Flow rate, $Q = \frac{V}{t}$

Uncertainty in calculated flow rate,

$$w_Q = \left[ \left( \frac{\partial Q}{\partial V} w_V \right)^2 + \left( \frac{\partial Q}{\partial t} w_t \right) \right]^{\frac{1}{2}}$$

$$= \left[ \left( \frac{1}{t} w_V \right)^2 + \left( -\frac{V}{t^2} w_t \right)^2 \right]^{\frac{1}{2}}$$

$$= \left[ \left( \frac{1}{27.09} \times 5 \times 10^{-6} \right)^2 + \left( -\frac{1 \times 10^{-3}}{27.09^2} \times 0.1 \right)^2 \right]^{\frac{1}{2}}$$

$$= 2.294 \times 10^{-7}\ m^3 / s$$

Flow rate, $Q = 7.3828 \times 10^{-5} \pm 2.294 \times 10^{-7}\ m^3/s$

$$Velocity, v = \frac{Q}{A}$$

Cross Sectional area of tube, A

$$A = \frac{\pi D^2}{4}$$

$$= \frac{\pi \times .005^2}{4}$$

$$= 1.9635 \times 10^{-5}\ m^2$$

Uncertainty in calculated area,

$$w_A = \frac{\partial A}{\partial D} w_D$$

$$= \frac{\pi \times 2 \times D \times w_D}{4}$$

$$= \frac{\pi \times 2 \times .005 \times .00001}{4}$$

$$= 7.854 \times 10^{-8}\ m^2$$

Uncertainty in calculated velocity,

$$w_V = \left[\left(\frac{\partial v}{\partial A} w_A\right)^2 + \left(\frac{\partial v}{\partial Q} w_Q\right)^2\right]^{\frac{1}{2}}$$

$$= \left[\left(-\frac{Q}{A^2} w_A\right)^2 + \left(\frac{1}{A} w_Q\right)^2\right]^{\frac{1}{2}}$$

$$= \left[\left(-\frac{7.3826\times10^{-5}\times7.854\times10^{-8}}{\left(1.9635\times10^{-5}\right)^2}\right)^2 + \left(\frac{1\times2.294\times10^{-7}}{1.9635\times10^{-5}}\right)^2\right]^{\frac{1}{2}}$$

$$= 0.01904 m/s$$

$$Velocity, v = 3.760019 \pm 0.01904 m/s$$

$$Viscosity, \mu = \frac{1}{a + bT + cT^2 + dT^3}$$ Here T is in ºC

$$= \frac{1}{557.82468 + 19.408782\times25 + .1360459\times25^2 - 3.1160832\times10^{-4}\times20^3}$$

$$= 1.002078\times10^{-3} N - s/m^2$$

Uncertainty in calculated viscosity

$$w_\mu = \frac{\partial \mu}{\partial \mathrm{T}} w_T$$

$$= \frac{b + 2cT + 3dT^2}{\left(a + bT + cT^2 + dT^3\right)^2} w_T$$

$$= \frac{19.408782 + 2\times.1360459\times25 - 3.1160832\times10^{-4}\times25^2}{\left(557.83468 + 19.408782\times25 + 0.1360459\times25^2 - 3.1160832\times10^{-4}\times25^3\right)^2}\times1$$

$$= 2.06215\times10^{-5}$$

$$Viscosity, \mu = 1.002078\times10^{-3} \pm 2.06215\times10^{-5} N - s/m^2$$

Reynolds no. Re, = $\frac{\rho v D}{\mu}$

Uncertainty in calculated Reynolds no.

$$w_{\mathrm{Re}} = \left[ \left( \frac{\partial \mathrm{Re}}{\partial \rho} w\rho \right)^2 + \left( \frac{\partial \mathrm{Re}}{\partial v} w_v \right)^2 + \left( \frac{\partial \mathrm{Re}}{\partial D} w_D \right)^2 + \left( \frac{\partial \mathrm{Re}}{\partial \mu} w_\mu \right)^2 \right]^{\frac{1}{2}}$$

$$= \left[ \left( \frac{vD}{\mu} w_\rho \right)^2 + \left( \frac{\rho D}{\mu} w_v \right)^2 + \left( \frac{\rho v}{\mu} w_D \right)^2 + \left( -\frac{\rho v D}{\mu^2} w_\mu \right)^2 \right]^{\frac{1}{2}}$$

$$= \left[ \begin{array}{l} \left( \frac{3.760019 \times .005}{1.002078 \times 10^{-3}} \times (-0.66875) \right)^2 + \left( \frac{991.25 \times .005}{1.002078 \times 10^{-3}} \times .01904 \right)^2 + \\ \left( \frac{991.25 \times 3.760019}{1.00278 \times 10^{-3}} \times .0001 \right)^2 + \left( -\frac{991.25 \times 3.760019 \times .005}{\left(1.00278 \times 10^{-3}\right)^2} \times 2.06215 \times 10^{-5} \right)^2 \end{array} \right]^{\frac{1}{2}}$$

$$= 536.168$$

Reynolds no. Re,= 23269.85±536.168

Theoretical straight friction factor,

$$f_s = .0791 \times \mathrm{Re}^{-0.25}$$

Uncertainty in the calculation of theoretical straight friction factor,

$$w_{f_s} = \frac{\partial f_s}{\partial \mathrm{Re}} w_{\mathrm{Re}}$$
$$= 0.0791 \times (-0.25) \times \mathrm{Re}^{-1.25}\ w_{\mathrm{Re}}$$
$$= 0.0791 \times (-0.25) \times 23269.85^{-1.25} \times 536.168$$
$$= -3.689 \times 10^{-5}$$

Theoretical straight friction factor, $f_S = 6.3982 \times 10^{-3} \pm 3.689 \times 10^{-5}$

Experimental straight friction factor, $f_s = \frac{2h_{st} gD}{4L_{st} v^2}$

Uncertainty in the calculation of experimental straight friction factor,

$$w_{f_s} = \left[ \left( \frac{\partial f_s}{\partial h_{st}} w_{h\,st} \right)^2 + \left( \frac{\partial f_s}{\partial D} w_D \right)^2 + \left( \frac{\partial f_s}{\partial v} w_v \right)^2 + \left( \frac{\partial f_s}{\partial L_{st}} w_{L_{st}} \right)^2 \right]^{\frac{1}{2}}$$

$$= \left[ \left( \frac{gD}{2v^2 L_{st}} w_{h_{st}} \right)^2 + \left( \frac{gh_{st}}{2v^2 L_{st}} w_D \right)^2 + \left( -\frac{gDh_{st}}{v^2 L_{st}} w_v \right)^2 + \left( \frac{gDh_{st}}{v^2 L_{st}} w_{L_{st}} \right)^2 \right]^{\frac{1}{2}}$$

$$= \left[ \begin{array}{l} \left( \frac{9.81 \times .005}{2 \times 3.760019^2 \times 0.50} \times 0.0005 \right)^2 + \left( \frac{9.81 \times 0.2438}{2 \times 3.760019^2 \times 0.50} \times .0001 \right)^2 + \\ \left( -\frac{9.81 \times .005 \times 0.2438}{3.760019^2 \times .50} \times 0.01904 \right)^2 + \left( \frac{9.81 \times .005 \times 0.2438}{3.760019^2 \times 0.50} \times 0.001 \right)^2 \end{array} \right]^{\frac{1}{2}}$$

$$= 1.7408 \times 10^{-5}$$

Experimental straight friction factor, $f_s = 6.6392 \times 10^{-3} \pm 1.7408 \times 10^{-5}$

Bending friction factor,

$$f_B = \frac{\Delta P_{13} - \frac{4L_{st}\rho v^2 f_s}{2D}}{\frac{4L_c \rho v^2}{2D}}$$

$$= .041773 \times \frac{\Delta P_T \times D}{\rho v^2} - .8355 L_{st} \times f_s$$

Here $L_c = 15 \times \pi \times .0254$ m

$L_{st} = (100+60+130)D+14L$ , $L$= Spacer length

Bend friction factor, $f_B = 8.377 \times 10^{-3} \pm 8.0006 \times 10^{-4}$

Uncertainty in the calculation of bend friction factor,

$$w_{f_B} = \left[ \begin{array}{l} \left( \frac{\partial f_B}{\partial \Delta P_T} w_{\Delta P_T} \right)^2 + \left( \frac{\partial f_B}{\partial D} w_D \right)^2 + \left( \frac{\partial f_B}{\partial v} w_v \right)^2 + \left( \frac{\partial f_B}{\partial L_{st}} w_{L\,st} \right)^2 + \\ \left( \frac{\partial f_B}{\partial f_s} w_{f\,s} \right)^2 + \left( \frac{\partial f_B}{\partial \rho} w_\rho \right)^2 \end{array} \right]^{\frac{1}{2}}$$

$$= \left[ \begin{array}{l} \left( \frac{0.41773 \times .005}{991.25 \times 3.760019^2} \times 8.25 \right)^2 + \left( \frac{0.41773 \times 124920.61}{991.25 \times 3.760019^2} \times .0001 \right)^2 + \\ \left( -\frac{0.41773 \times 124920.61 \times .005 \times 2}{991.25 \times 3.760019^3} \times 0.01904 \right)^2 + \left( -0.8355 \times 1 \times 10^{-3} \times 6.6392 \times 10^{-3} \right)^2 + \\ \left( -0.8355 \times 2.1612 \times 1.7408 \times 10^{-5} \right)^2 + \left( -1 \times \frac{0.41773 \times 124920.61 \times 0.005}{991.25^2 \times 3.760019^2} \times 0.66875 \right)^2 \end{array} \right]^{\frac{1}{2}}$$

$$= 8.0006 \times 10^{-4}$$